

AD614707

DMIC Report 214  
March 1, 1965

# OXIDATION OF NICKEL - AND COBALT-BASE SUPERALLOYS

37-P

COPY	11	OF	12	92
HARD COPY	\$ . 2.00			
MICROFICHE	\$ . 0.50			

DDC

MAY 11 1965

DEFENSE METALS INFORMATION CENTER  
Battelle Memorial Institute  
Columbus, Ohio 43201

ARCHIVE COPY

The Defense Metals Information Center was established at Battelle Memorial Institute at the request of the Office of the Director of Defense Research and Engineering to provide Government contractors and their suppliers technical assistance and information on titanium, beryllium, magnesium, aluminum, refractory metals, high-strength alloys for high-temperature service, corrosion- and oxidation-resistant coatings, and thermal-protection systems. Its functions, under the direction of the Office of the Director of Defense Research and Engineering, are as follows:

1. To collect, store, and disseminate technical information on the current status of research and development of the above materials.
2. To supplement established Service activities in providing technical advisory services to producers, melters, and fabricators of the above materials, and to designers and fabricators of military equipment containing these materials.
3. To assist the Government agencies and their contractors in developing technical data required for preparation of specifications for the above materials.
4. On assignment, to conduct surveys, or laboratory research investigations, mainly of a short-range nature, as required, to ascertain causes of troubles encountered by fabricators, or to fill minor gaps in established research programs.

Contract No. AF 33(615)-1121  
Project No. 8975

*Roger J. Runck*

Roger J. Runck  
Director

"The information in this report came from many sources, and the original language may have been extensively quoted. Quotations should credit the original authors and the originating agency. Where patent questions appear to be involved, the usual preliminary search is advised before making use of the material, and where copy-righted material is used, permission should be obtained for its further publication."

COPIES AVAILABLE FROM OTS \$

**CLEARINGHOUSE FOR FEDERAL SCIENTIFIC AND TECHNICAL INFORMATION, CFSTI  
INPUT SECTION 410.11**

**LIMITATIONS IN REPRODUCTION QUALITY OF TECHNICAL ABSTRACT BULLETIN  
DOCUMENTS, DEFENSE DOCUMENTATION CENTER (DDC)**

*AD 614 707*

- ☐ 1. AVAILABLE ONLY FOR REFERENCE USE AT DDC FIELD SERVICES.  
COPY IS NOT AVAILABLE FOR PUBLIC SALE.
- ☒ 2. AVAILABLE COPY WILL NOT PERMIT FULLY LEGIBLE REPRODUCTION.  
REPRODUCTION WILL BE MADE IF REQUESTED BY USERS OF DDC.
  - ☒ A. COPY IS AVAILABLE FOR PUBLIC SALE.
  - ☐ B. COPY IS NOT AVAILABLE FOR PUBLIC SALE.
- ☐ 3. LIMITED NUMBER OF COPIES CONTAINING COLOR OTHER THAN BLACK  
AND WHITE ARE AVAILABLE UNTIL STOCK IS EXHAUSTED. REPRODUCTIONS  
WILL BE MADE IN BLACK AND WHITE ONLY.

**TSL-121-2/64**

**DATE PROCESSED:**

**PROCESSOR:**

*5-13-65  
G. Lee*

DMIC Report 214  
March 1, 1965

OXIDATION OF NICKEL-AND COBALT-BASE  
SUPERALLOYS

by

C. H. Lund and H. J. Wagner

to

OFFICE OF THE DIRECTOR OF DEFENSE  
RESEARCH AND ENGINEERING

DEFENSE METALS INFORMATION CENTER  
Battelle Memorial Institute  
Columbus, Ohio 43201

The new high-strength nickel-base alloys with chromium contents of about 10 percent do not have adequate oxidation resistance over their useful temperature range and require protective coatings.

Elements which promote oxidation resistance in super-alloys are chromium, silicon, aluminum, and several of the rare earths, especially cerium.

Boron adversely affects oxidation resistance; so do titanium, molybdenum, and tungsten if over 0.5 percent.

Oxidation can be beneficial if it produces a uniform adherent protective surface film, or if it produces a film used to alter surface properties, such as to increase emissivity.

## TABLE OF CONTENTS

	<u>Page</u>
SUMMARY . . . . .	i
INTRODUCTION . . . . .	1
FUNDAMENTALS OF THE OXIDATION OF Ni-Cr AND Co-Cr ALLOYS . . . . .	1
GENERAL SURFACE OXIDATION . . . . .	3
Experimental Methods . . . . .	4
Oxidation of Superalloys . . . . .	4
INTERGRANULAR OXIDATION . . . . .	16
Alloy Depletion Effects . . . . .	21
OTHER SUBSURFACE OXIDATION . . . . .	22
EFFECT OF STRESS . . . . .	23
REFERENCES . . . . .	25

## APPENDIX

ALLOY INDEX AND COMPOSITIONS . . . . .	A-1
--	-----

# OXIDATION OF NICKEL- AND COBALT-BASE SUPERALLOYS

by

C. H. Lund\* and H. J. Wagner\*\*

## SUMMARY

The superalloys are oxidation resistant but all will oxidize at high temperatures when oxygen is present. The rate of oxidation will depend upon many factors including alloy composition, temperature, oxygen concentration, diffusion rates, etc. Alloys designed for maximum strength will not have maximum oxidation resistance. Therefore, the application of superalloys is a compromise between strength and oxidation considerations. When maximum strength and oxidation resistance are both desired, protective coatings are needed.

Superalloys are very complex nickel- or cobalt-base alloys containing closely controlled amounts of several elements. Each of these elements can participate in the oxide formation during high-temperature exposure, their participation being regulated by activation energy, diffusion, and heat of formation of the oxides.

General surface oxidation is the formation of an oxide layer of relatively uniform thickness on the surface of the alloy. Light surface oxidation is often not objectionable and may even be beneficial. Intergranular oxidation, on the other hand, can be a serious problem on thin sections or wire when present in only small amounts. The penetration of the oxide front not only reduces the effective cross section, but it can act as a notch to reduce fatigue resistance. It can also be very serious in notch-sensitive materials. Fortunately, intergranular oxidation takes place only at relatively high temperatures. Superalloys, particularly the precipitation-hardenable nickel-base alloys, are susceptible to intergranular oxide penetration.

Intergranular oxidation is preceded by alloy depletion ahead of the advancing oxide front. The compositional gradient that is produced can act as the driving force for continued metal-ion diffusion. The depleted zone also is weaker than the basic alloy, particularly in precipitation-hardenable nickel-base alloys where chromium, aluminum, and titanium are preferentially oxidized because of their relatively high affinity for oxygen. Loss of titanium and aluminum content is particularly detrimental to strength properties.

Unusual conditions of atmosphere or metal surface can result in subsurface oxidation not usually found in superalloys. For example, internal preferential oxidation of chromium rather than nickel might occur in atmospheres that are oxidizing to chromium and reducing to nickel, or internal oxidation might take place under a surface that has been previously carburized. Parameters for internal oxidation are not clearly defined.

Stress has an effect on the rate of oxidation. It appears that oxidation proceeds at a constant rate with increasing stress until a "critical" stress level is reached at which oxidation proceeds much more rapidly. Stress also produces spalling of even the tightly adherent oxides of most superalloys when sufficient shear is produced at the metal-oxide interface to cause cracking. Under these conditions oxidation is rapid as fresh metal is continuously being exposed for further reaction.

\*Chief Development Metallurgist, Martin Metals Company, Wheeling, Illinois.

\*\*Ferrous and High Alloy Metallurgy Research Division, Battelle Memorial Institute, Columbus, Ohio.

## INTRODUCTION

All of the superalloys will oxidize at high temperatures when oxygen is present in the enveloping atmosphere. The rate of oxidation depends upon alloy composition, temperature, oxygen concentration, oxides formed, diffusion rates of the metals in both base metal and oxide, diffusion rate of oxygen in the oxide, solubility of oxygen in the matrix, and a host of other variables. Oxidation may produce a general, uniform surface layer, or it may occur as intergranular penetration along the grain boundaries, as subsurface preferential oxidation (so-called "internal oxidation"), or as all three combined.

The effects of oxidation can be beneficial, or they can be harmful to the extent of causing catastrophic failure. Examples of beneficial oxides are the black oxides deliberately formed on the René 41\* skin of Mercury space capsules and on the Inconel X (presently designated Inconel alloy X-750) skin of X-15 research aircraft. These oxides are formed to increase the emissivity of the surface and thus help to dissipate the tremendous amounts of heat generated on the metal surfaces during reentry and high-speed flight. Catastrophic failure from oxidation occurs in thin sheets and fine wires subjected to temperatures too high for even short-time exposure. Other examples are given later in this report.

In general, the oxidation resistance of the nickel- and cobalt-base alloys is considered to be relatively good. The oxides formed are tightly adherent and protective. This is especially true of the simple solid-solution type of alloys up to temperatures in excess of 2000 F and of most other alloys at temperatures up to about 1850 F. Above this temperature, oxidation becomes a problem in the more complex superalloys. Additions of many of the elements that give the alloys elevated-temperature strength (e. g., titanium and molybdenum) decrease the oxidation resistance. Aluminum, too, when participating in the formation of certain strengthening phases, such as gamma prime, may promote decreased oxidation resistance even though it is generally a beneficial element when in solid solution.

We are concerned not only with the problem of oxidation of nickel- and cobalt-base alloys under service conditions, but also with the control of oxidation during melting, the importance of which is shown by the interest in recent years in vacuum and protective atmosphere melting of nickel-base superalloys. Because nickel-base alloys contain large amounts of such highly reactive elements as aluminum and titanium, they

are highly susceptible to the formation of oxide skins and films during melting and casting. Cobalt-base alloys on the other hand do not, as a rule, depend upon the precipitation of an aluminum-titanium-bearing compound for their strength and thus are not nearly as susceptible to oxide formation during melting and casting. Thus, vacuum melting and casting are considered beneficial for only a few of the cobalt-base superalloys.

## FUNDAMENTALS OF THE OXIDATION OF Ni-Cr AND Co-Cr ALLOYS

The superior oxidation resistance of nickel-chromium alloys has been recognized for over 50 years. Among the first to recognize this fact was Marsh, whose 1906 patent describes the important contribution of chromium when added to nickel. Nickel-chromium alloys containing about 20 per cent chromium have been standard for many years in applications where electrical resistance, particularly at high temperatures, is important. These alloys also served as the basis of the first superalloys, when it was discovered that they could be made precipitation hardenable by the addition of small amounts of titanium or aluminum, or both. In recent years, there has been a tendency, among those engaged in superalloy development, to retain only a minimum of chromium, an amount just sufficient to provide adequate resistance to oxidation and sulfidation. Whereas the early nickel-base superalloys contained 16-20 per cent chromium, the later ones contain 10-15 per cent, a portion of the chromium being displaced by elements contributing more to strength but less to oxidation resistance. The influence of chromium on the oxidation resistance of nickel is shown in Figure 1<sup>(1)\*</sup> and Table 1<sup>(2)</sup>.

Cobalt-base superalloys also contain a relatively high proportion of chromium, usually about 20 to 25 per cent. One of the reasons for the use of chromium is shown in Figure 2, which illustrates the oxidation rate as a function of chromium content<sup>(3)</sup>.

Simple binary nickel-chromium alloys have excellent oxidation resistance, provided sufficient chromium is present. Thus, Figure 1 shows that additions of up to 5 per cent chromium actually decrease the oxidation resistance at all temperatures up to 1200 C (2200 F) and that further additions of chromium are required to reverse the trend and impart superior oxidation resistance. Figure 1 also shows that some minimum amount of chromium is necessary to insure good corrosion resistance at various temperatures, the amount increasing from about 12 per cent at 900 C (1650 F) to about 18 per cent at 1200 C (2200 F). Similar data are given in Table 1, taken from work by

\*Compositions are given in the Appendix.

Throughout this report the trade names used are the ones current at the time of the investigation.

\*References are given on page 25.

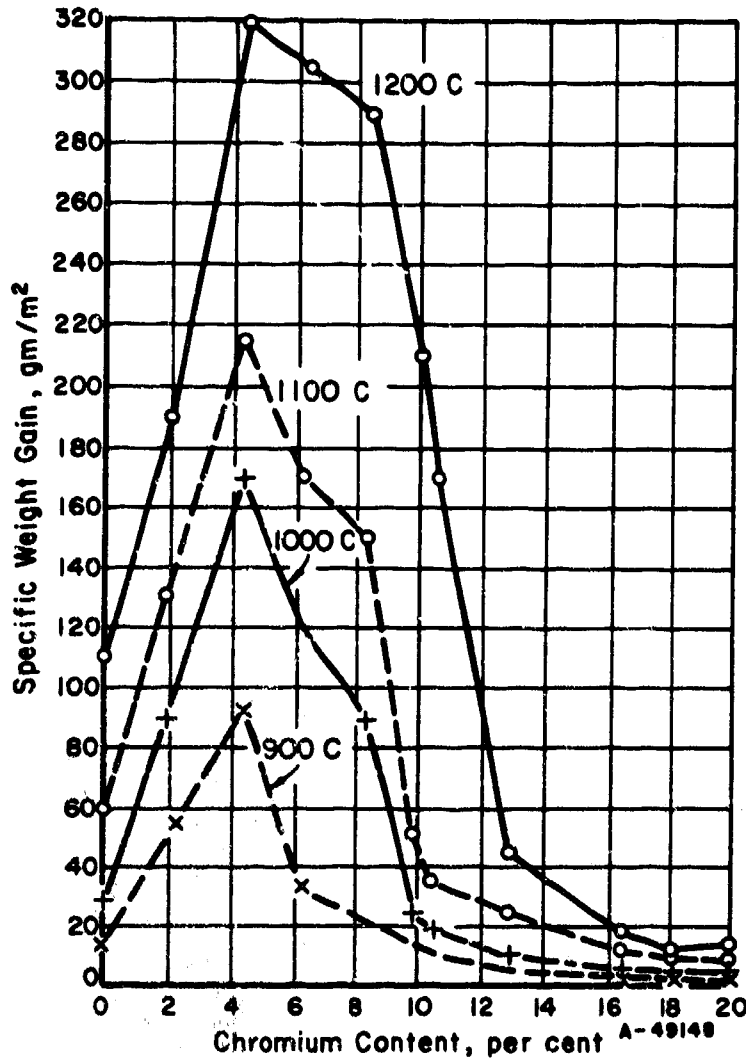


FIGURE 1. DEPENDENCE OF DEGREE OF OXIDATION ON THE CHROMIUM CONTENT OF BINARY Ni-Cr ALLOYS<sup>(1)</sup>

Specimens held 8 hours at temperature.

Zima<sup>(2)</sup>, which shows that the oxidation rate increases with increasing chromium content up to about 7.5 per cent chromium and then rapidly decreases between 7.5 and 11.1 per cent. Between 11.1 and 20.0 per cent chromium, there is a gradual decrease in oxidation rate with a minimum at 20 per cent. The behavior of the cobalt-chromium system, shown by the curves in Figure 2, is similar to that of the nickel-chromium system.

The chemical nature of the oxide films formed on nickel-base and cobalt-base alloys containing chromium varies with temperature and with chromium content. Chromium oxide ( $\text{Cr}_2\text{O}_3$ ), nickel oxide ( $\text{NiO}$ ), and cobalt oxide ( $\text{CoO}$ ), are the stable oxides usually found in the oxide scales of nickel-chromium and cobalt-chromium alloys. The actual composition of the oxide layers changes with temperature and time. In certain alloys with the base composition 80Ni-20Cr, it has been reported that  $\text{NiO}$  is the first oxide to form at low temperatures (approximately 750 to 930 F) after short periods of time<sup>(4,5,6)</sup>, or at about 2150 F

TABLE 1. OXIDATION DATA FOR NICKEL-CHROMIUM ALLOYS<sup>(2)</sup>

1096 C (2000 F)  
76 cm Hg of  $\text{O}_2$

Alloy	Wt % Cr	At % Cr	$K_p$ ( $\text{g}^2\text{cm}^{-4}\text{sec}^{-1}$ )	$K_p/K_{p0}$
1	0.00	0.00	$5.48 \times 10^{-10}$	1.00
2	0.32	0.36	$23.6 \times 10^{-10}$	4.30
3	0.92	1.04	$29.7 \times 10^{-10}$	5.42
4	2.00	2.25	$39.6 \times 10^{-10}$	7.22
5	3.45	3.88	$46.8 \times 10^{-10}$	8.55
6	5.67	6.37	$58.5 \times 10^{-10}$	10.7
7	7.64	8.55	$67.8 \times 10^{-10}$	12.4
8	8.71	9.70	$30.8 \times 10^{-10}$	5.63
9	11.10	12.20	$3.79 \times 10^{-10}$	0.69
10	14.90	16.50	$0.35 \times 10^{-10}$	0.064
	20.0	22.0	0.07	0.013(a)

(a) Given in private communication by Dr. E. A. Gulbransen of The Westinghouse Research Laboratory.

$K_p$  = parabolic rate constant for alloy  
 $K_{p0}$  = parabolic rate constant for nickel

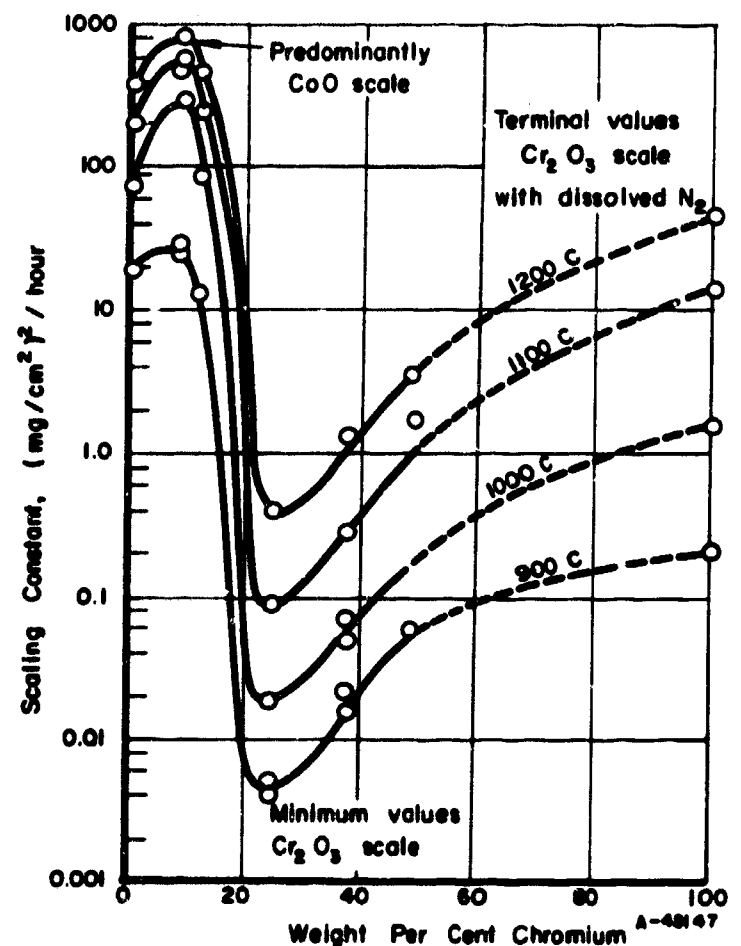


FIGURE 2. FIRST PARABOLIC SCALING CONSTANT VERSUS ALLOY COMPOSITION FOR Co-Cr ALLOYS HEATED IN AIR<sup>(3)</sup>



after long oxidation times and cyclic heating.<sup>(4)</sup> Between 930 F and 1300 F,  $\text{Cr}_2\text{O}_3$  has been observed to form. At higher temperatures around 1650-1750 F, complex double oxides are formed called spinels. For nickel-base alloys, the spinel is usually designated as  $\text{NiO} \cdot \text{Cr}_2\text{O}_3$  or as  $\text{NiCr}_2\text{O}_4$ . At high temperatures the oxides formed are in two layers, an inner layer of  $\text{Cr}_2\text{O}_3$  adjacent to the metal, and an outer layer of spinel. The thickness of the spinel layer increases with time and temperature.

Spinel also are of varying composition, the  $\text{Cr}_2\text{O}_3$  content increasing with increasing time and temperature. According to Ignatov<sup>(5,6)</sup>, nickel-chromium spinels begin to decompose at temperatures between 1100 C (2010 F) and 1200 C (2190 F) into the components  $\text{NiO}$  and  $\text{CrO}$ . The decomposition of the spinels has an important influence on the oxidation process because it permits  $\text{CrO}$  to be vaporized from the surface, increasing the driving force for the diffusion of chromium through the oxide scale. Increased diffusion of chromium ions results in more oxidation.<sup>(7)</sup> In nickel-base alloys, the diffusion of nickel ions through the scale is negligible so that oxidation rates are dependent upon the rate of chromium diffusion. In cobalt-base alloys, the diffusion of cobalt ions is faster than that of chromium ions so that  $\text{CoO}$  is found in the outer oxide layers. Gradual buildup of  $\text{CrO}$  in the oxide scale results in an increasingly effective barrier against diffusion of cobalt ions, and hence a slowing down of the oxidation rate.<sup>(3)</sup> It is generally accepted that the composition of the oxide films is determined by the relative activation energies of diffusion of the alloy components and the heats of formation of the various oxides.<sup>(7)</sup> The reaction usually occurs by diffusion of the metal ions through the scale rather than by inward diffusion by oxygen. However, Ignatov states that oxygen diffusion inward is observed at temperatures of about 1000 C (1830 F) and up.<sup>(6)</sup>

Superalloys are very complex alloys containing closely controlled amounts of several elements. Each of these elements can participate in oxide formation during high-temperature exposure, their participation being regulated by activation energy, diffusion, and heat of formation of the oxides, as previously mentioned.

Some of the elements commonly present in superalloys are considered to be beneficial to oxidation resistance, i. e., they contribute to the formation of a stable oxide. Examples of these are silicon, aluminum, and several of the rare-earth elements, especially cerium. Aluminum plays the most important role. If aluminum is present in amounts of about 3 per cent or more (depending upon temperature), a spinel  $\text{NiO} \cdot \text{Al}_2\text{O}_3$  (or  $\text{NiAl}_2\text{O}_4$ ) is formed, which is mutually soluble with  $\text{NiO} \cdot \text{Cr}_2\text{O}_3$  ( $\text{NiCr}_2\text{O}_4$ ) at temperatures of about 1300 to 1900 F.<sup>(6)</sup> These spinel films are

very protective. Aluminum is also important in oxides formed at lower temperatures. When aluminum is present, a dense inner layer of  $\text{Al}_2\text{O}_3$  is formed. However, it does not always effectively slow down the diffusion of metallic ions through the metal-oxide interface to the outer surface, which would be necessary for improved protection of the alloy. Hagel<sup>(8)</sup> investigated a variety of iron-aluminum, iron-chromium-aluminum, nickel-aluminum, and cobalt-aluminum alloys at temperatures between 600 and 1350 C in low-pressure oxygen. He reported that the defect structure and metastability of  $\gamma\text{-Al}_2\text{O}_3$  are the principal reasons for the ineffectiveness of aluminum in preventing oxidation of these alloys. Below about 900 C,  $\gamma\text{-Al}_2\text{O}_3$  is formed, which permits the passage of nickel, cobalt, and iron ions through the layer, becoming oxidized to  $\text{NiO}$ ,  $\text{Co}_3\text{O}_4$ , and  $\text{Fe}_3\text{O}_4$ , respectively. The transformation from  $\gamma\text{-Al}_2\text{O}_3$  to  $\alpha\text{-Al}_2\text{O}_3$  occurs between 900 C and 1100 C, and is accompanied by volume changes which can cause fissuring of the scale. Above 1100 C the  $\alpha\text{-Al}_2\text{O}_3$  is effective in protecting iron. Some  $\text{NiO}$  and  $\text{NiAl}_2\text{O}_4$  may still form, but cobalt is not protected. The beneficial effect of chromium is due to the extension of the  $\alpha\text{-Al}_2\text{O}_3$  in solution with  $\alpha\text{-Cr}_2\text{O}_3$  down to 600 C.

Examples of elements that adversely affect the oxidation resistance of Ni-Cr alloys are boron (over 0.1 per cent), titanium, molybdenum, and tungsten (the latter three when over 0.5 per cent).<sup>(6)</sup>

According to the Soviet investigators, additions of cerium, thorium, and several of the rare earths improve the high-temperature oxidation resistance of the nickel-base superalloys by alloying with the  $\text{NiO} \cdot \text{Cr}_2\text{O}_3$  spinel and preventing the rapid vaporization of  $\text{Cr}_2\text{O}_3$  at temperatures of about 2000 F and above.<sup>(5)</sup>

#### GENERAL SURFACE OXIDATION

General surface oxidation can be defined as the formation of an oxide layer of relatively uniform thickness on the surface of the alloy. Most often, this type of oxidation is evaluated by measuring the weight change of a sample after a specified exposure time or continuously during the test. A weight gain may be the result of oxygen (and, sometimes, nitrogen) pick-up during oxidation, whereas a weight loss may be the result of spalling of the surface scale. When oxide scale is lost, the weight of the scale lost is the sum of the oxygen plus the metal contributing to the oxide formation.\* Because metal that is spalled must first be oxidized, it is possible for a metal or an alloy, at any given time, to show no net weight change (if adherent oxide weight gain equals loss

\*Intergranular oxidation or oxidation of a second phase may cause weight loss if grains are lost.

of metal in scale spalled), suggesting that the alloy is inert to its surroundings. Naturally, this would not be true.

### Experimental Methods

The above illustration serves to point up the need for great care in performing and in interpreting oxidation studies. Because of the many variables involved, it often is difficult to compare test results unless they are run under identical conditions. Temperature, oxygen partial pressure, and specimen surface roughness are just a few of the possible variables. If the oxide layer spalls off, weight-gain data can be quite erroneous. Probably the most reliable experimental method is to test the specimen in a refractory cup so that cup and contents can be weighed at intervals. In this manner, any scale falling from the specimen will be retained and weighed.

Some investigators choose to use mechanical or chemical methods for removing the oxide

formed during exposure. These methods, if properly carried out, result in a more direct indication of the amount of metal lost as a result of oxidation, than is indicated by weight-gain measurements. Accordingly, the data presented by different investigators for various alloys must be carefully analyzed in terms of test procedure used. In this report, experimental data obtained under essentially similar conditions have been plotted on the same graphs in order to compare results.

### Oxidation of Superalloys

Figures 3 and 4 show the oxidation resistance of the Nimonic family<sup>(9,10)</sup> of alloys plus a few data points for Haynes Stellite Alloy 31.<sup>(11)</sup> In these tests, the loss of metal by oxidation is indicated by the weight loss. Each specimen was descaled electrolytically in caustic soda after exposure. Before descaling, these alloys would have shown a weight gain. Figure 3 gives the results of oxidation during continuous

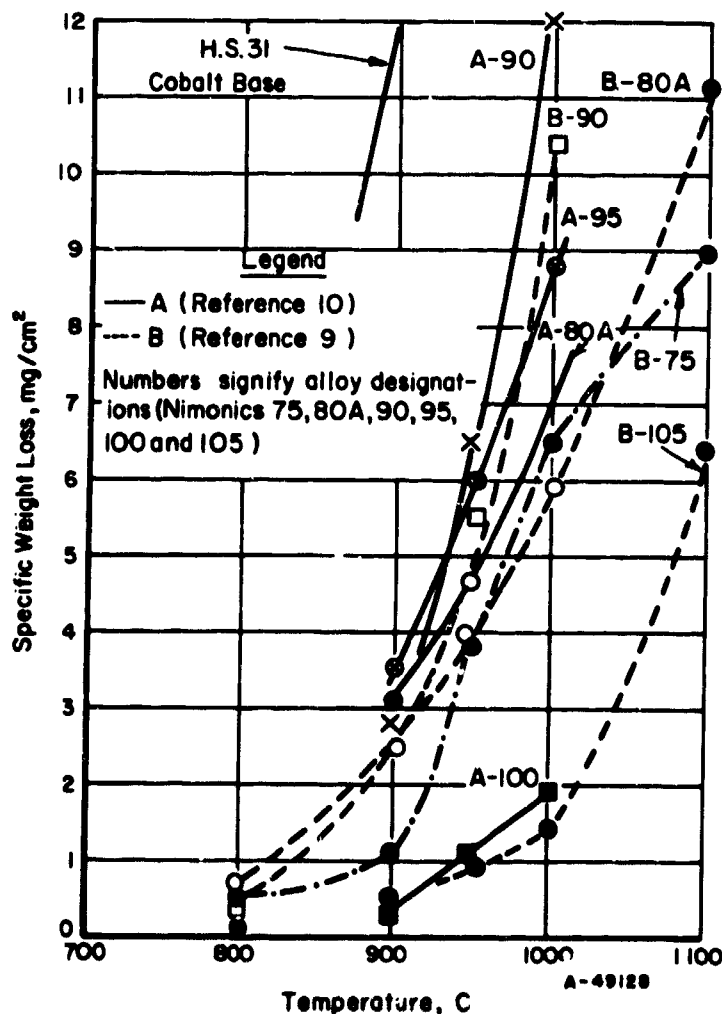


FIGURE 3. OXIDATION RESISTANCE OF NIMONIC ALLOYS DURING CONTINUOUS HEATING OF FOIL FOR 100 HOURS IN AIR

Weight loss determined after descaling electrolytically in caustic soda.

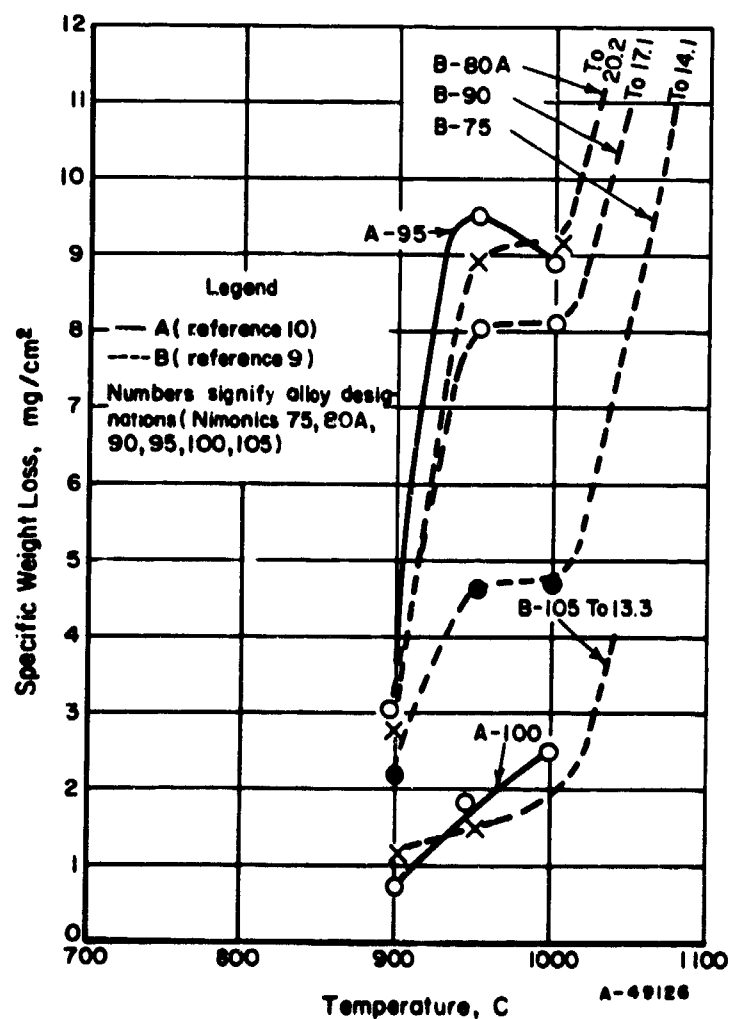


FIGURE 4. OXIDATION RESISTANCE OF NIMONIC ALLOYS DURING INTERMITTENT HEATING IN AIR FOR 100 HOURS, COOLED TO ROOM TEMPERATURE EVERY 24 HOURS

Weight loss determined after descaling electrolytically in caustic soda.

exposure to air for 100 hours at various temperatures, whereas Figure 4 gives data for specimens subjected to intermittent heating in air. For the latter test, each specimen was cycled from the test temperature to room temperature and back once every 24 hours. (9, 10)

Two items of importance are shown by these data: these are (1) the excellent resistance to oxidation of the nickel-base superalloys and

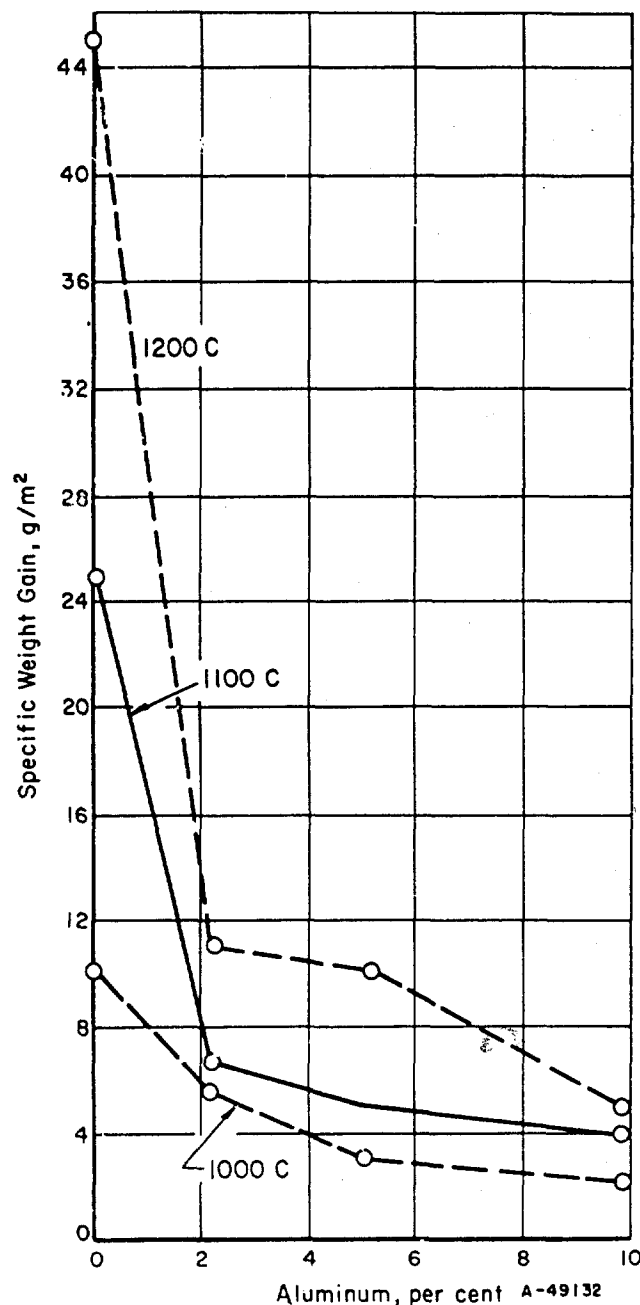


FIGURE 5. OXIDATION RESISTANCE OF NICKEL ALLOYS CONTAINING 12 PER CENT CHROMIUM AND VARIOUS AMOUNTS OF ALUMINUM<sup>(1)</sup>

Specimens held 8 hours at temperature.

(2) the marked increase in oxidation resistance imparted by aluminum. Nimonic Alloys 100 and 105 have about 5 per cent aluminum (also a low titanium content), whereas the other alloys have lower aluminum contents, 2 per cent or less (also higher titanium contents). Tūmarev and Panyushin<sup>(1)</sup> obtained similar results, as shown in Figures 5 and 6.

Figure 7 gives data for two of the newer nickel-base alloys, IN-100 and SM200. The data for IN-100 and SM200 are reported as a weight gain, indicating that the scale remained on the specimens. These data are for 2000 F.<sup>(12)</sup> Although lower temperature data are not available, it is expected that the alloys would show less difference in performance at temperatures under 2000 F.

Figure 8<sup>(13)</sup> illustrates the behavior of certain nickel-base alloys that were subjected to

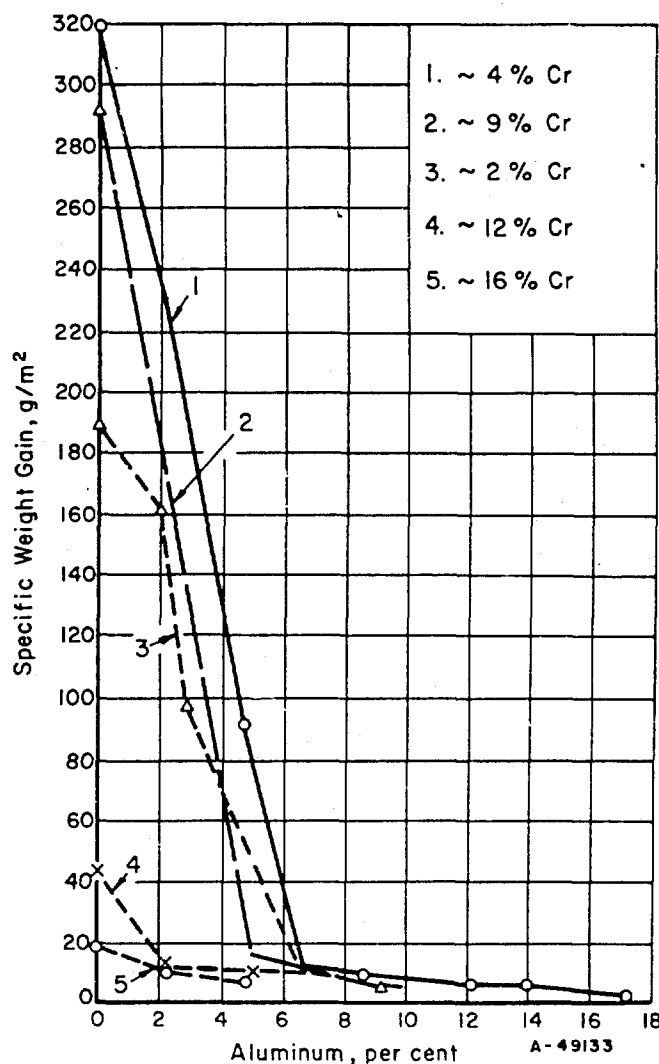


FIGURE 6. OXIDATION RESISTANCE OF ALLOYS CONTAINING VARIOUS AMOUNTS OF CHROMIUM AND ALUMINUM<sup>(1)</sup>

Specimens held 8 hours at temperature.

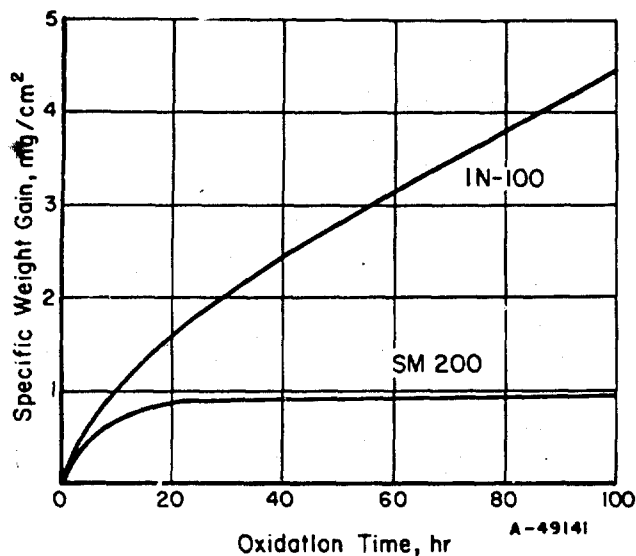


FIGURE 7. OXIDATION BEHAVIOR OF SM200 AND IN-100 AT 2000 F<sup>(12)</sup>

intermittent heating. It was assumed that if the specimens showed a weight loss it was because all the oxide scale had spalled off. The likelihood was discounted that simultaneous weight gain from oxidation and partial spalling would account for low losses or gains in weight. For these experiments, an intermittent heating cycle consisted of inserting a rack of test specimens for 15 minutes into a furnace held at the test temperature and then removing the rack for 5 minutes. This cycle was repeated 3000 times, for a total elapsed time of 1000 hours.

Figure 9<sup>(14)</sup> shows some of the data from the same work, comparing the resistance to spalling of several nickel-base and iron-base alloys. It must be borne in mind that the percentage loss in

TABLE 2. DEPTH OF OXIDE PENETRATION OF SOME ALLOYS AFTER 1000 HOURS OF CYCLIC EXPOSURE IN AIR AT 1800 F

Alloy	Penetration After 3000 Cycles to 1800 F (1000 hr.), in.
Nimonic 75	0.005
Inconel (Pre-1951)	0.012
AISI Type 330 Steel	0.0050
Incoloy	0.0062
AISI Type 310 Steel	0.0052
AISI Type 309 Steel	0.0064

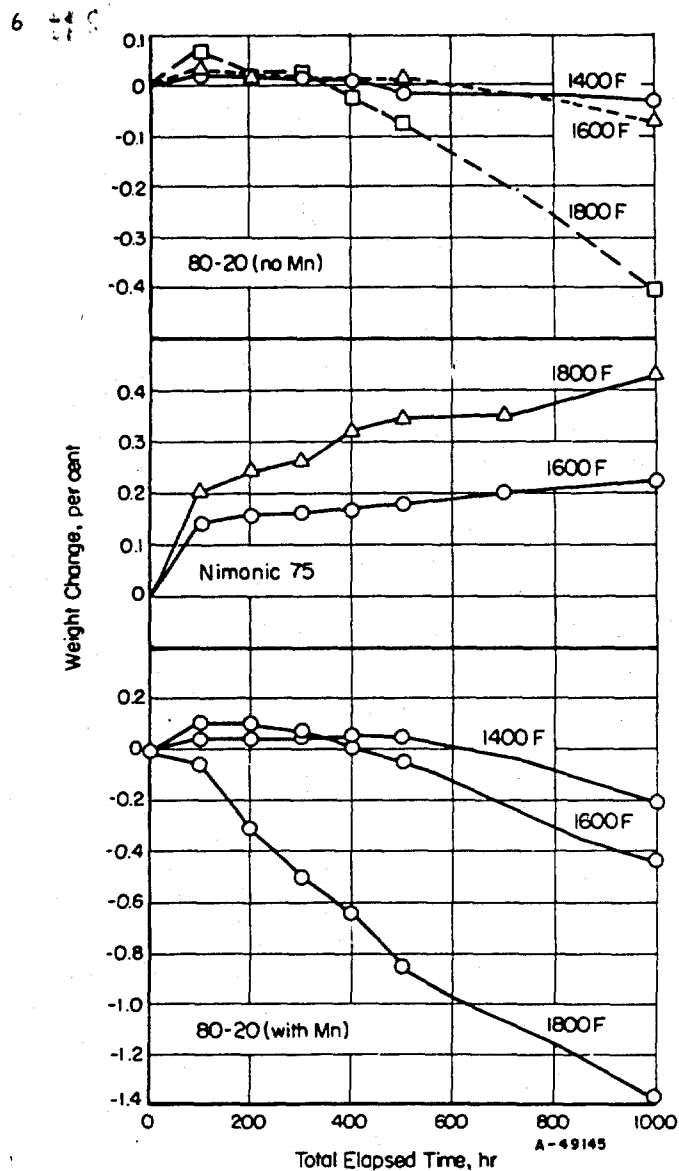


FIGURE 8. BEHAVIOR OF NICKEL ALLOYS DURING INTERMITTENT HEATING<sup>(13)</sup>

Specimens inserted in furnace for 15 minutes, removed from furnace for 5 minutes. Total elapsed time, 20 minutes per cycle. Specimen size, 0.031 in. x 3/4 in. x 3 in.

weight due to spalling is always higher than is the gain in weight observed when the scale is adherent. This is because, in the first case, the loss is due to metal loss, but the weight gain is due to oxygen. Accordingly, it is instructive to look also at the depth of penetration, calculated from a comparison of the original thickness with the thickness of unattacked metal remaining after the test. Table 2 shows these data for the 1800 F exposure. It is clear from these data that Nimonic 75, Types 330, 310, 309, and Incoloy were nearly alike in terms of penetration, a fact not evident in Figure 9.

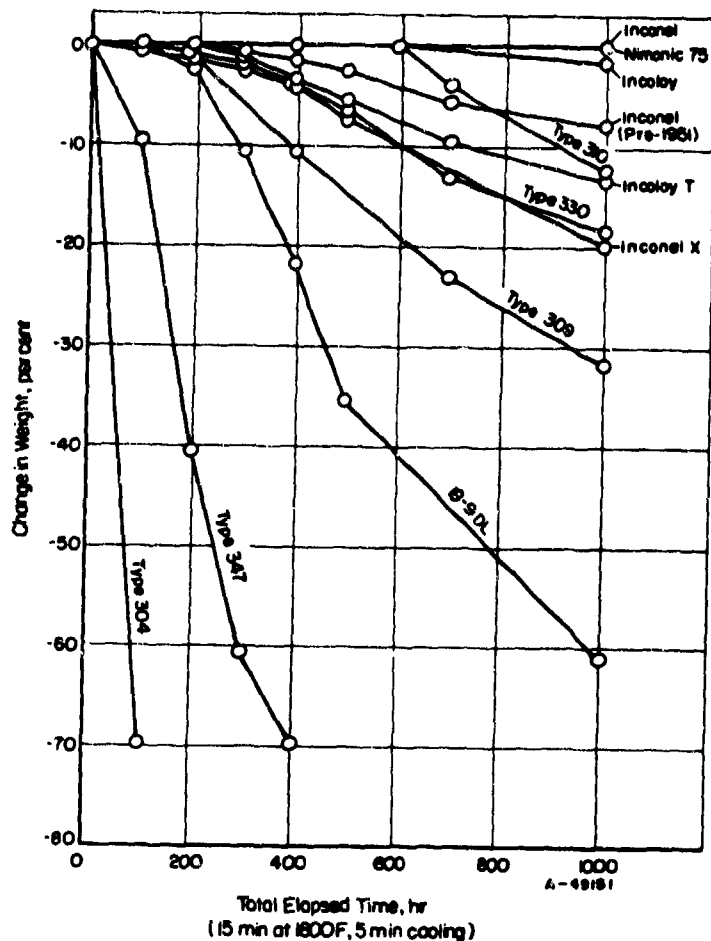


FIGURE 9. BEHAVIOR OF SEVERAL NICKEL-BASE AND IRON-BASE ALLOYS DURING INTERMITTENT HEATING<sup>(14)</sup>

See Figure 8 for details about test.

Figure 10<sup>(14)</sup> shows the relative oxidation characteristics of several alloys after exposure to slow-moving air at various temperatures. No details of test procedure or sheet thickness were given in the source, so the data can be used for comparison purposes only.

Scaling of René 41 sheet was reported by Childers and Simenz<sup>(15)</sup> for temperatures between 1650 and 2000 F. Figure 11 summarizes the effect of time and temperature on the scale thickness for 0.010-inch-thick sheet heated in air.

Scaling and subscale reactions in René 41 sheet and cast Udimet 700 were recently reported by Wlodek<sup>(16)</sup> for the temperature range 1600 F to 2000 F. Figures 12 and 13 show the results for solution-annealed material on a log-log plot, and indicate the change from linear to parabolic rates. Figures 14 and 15 show the linear portions on a linear plot, and also indicate that the rates for aged material and annealed material may be different. Subscale reactions are discussed later in the present report, under the section covering alloy depletion effects.

Measurements of the change in thickness of René 41 sheet specimens exposed for 50 hours to

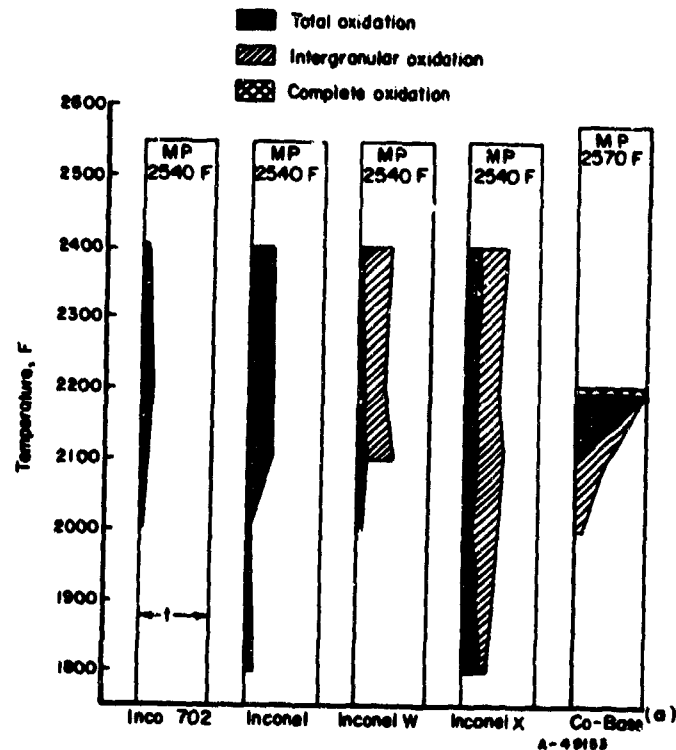


FIGURE 10. COMPARATIVE OXIDATION CHARACTERISTICS OF HIGH-TEMPERATURE SHEET ALLOYS<sup>(14)</sup>

Cross-sectional loss in thickness after 100-hour exposure to a slow-moving air atmosphere.  $t$ , the thickness of the sheet, was not given. The data are for comparative purposes only.

(a) This alloy was not identified in the paper. However, it can be assumed that it is L-605 (Haynes Alloy 25).

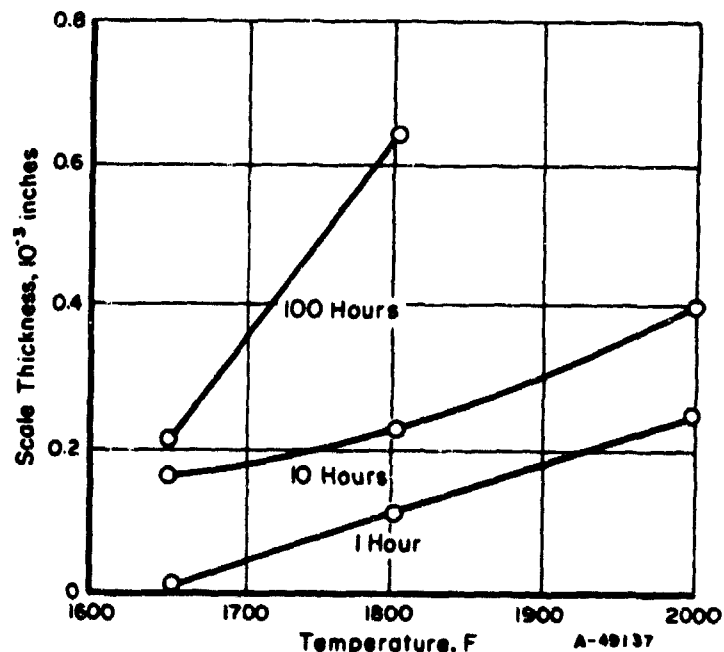


FIGURE 11. EFFECT OF TIME AND TEMPERATURE ON SCALE THICKNESS IN 0.010 IN. RENÉ 41 HEATED IN AIR<sup>(15)</sup>

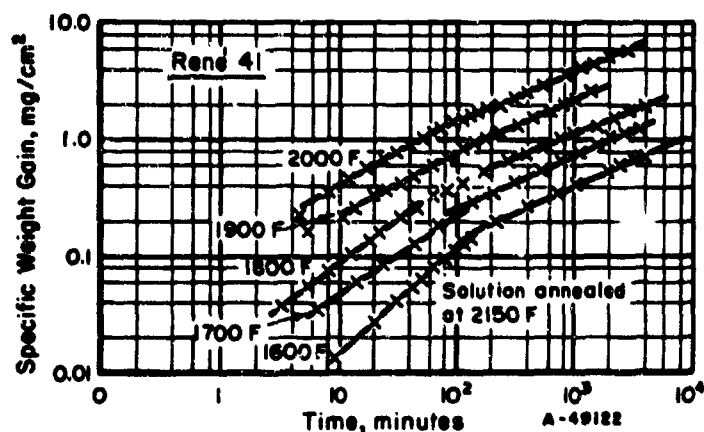


FIGURE 12. LOGARITHMIC PLOT OF SPECIFIC WEIGHT GAIN AGAINST TIME FOR A SINGLE HEAT OF RENÉ 41 SHEET<sup>(16)</sup>

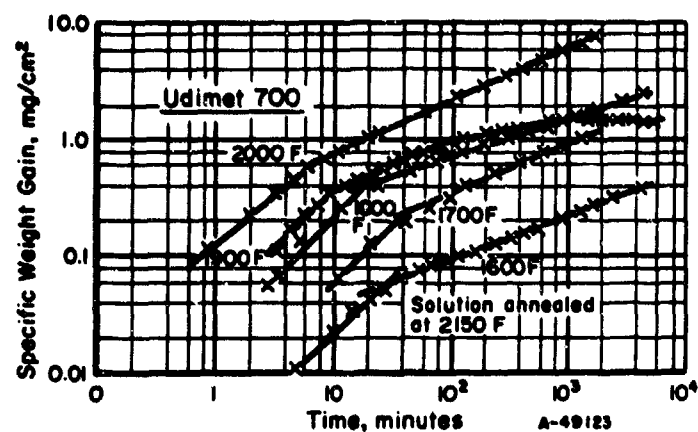


FIGURE 13. LOGARITHMIC PLOT OF SPECIFIC WEIGHT GAIN AGAINST TIME FOR A SINGLE HEAT OF CAST UDIMET 700<sup>(16)</sup>

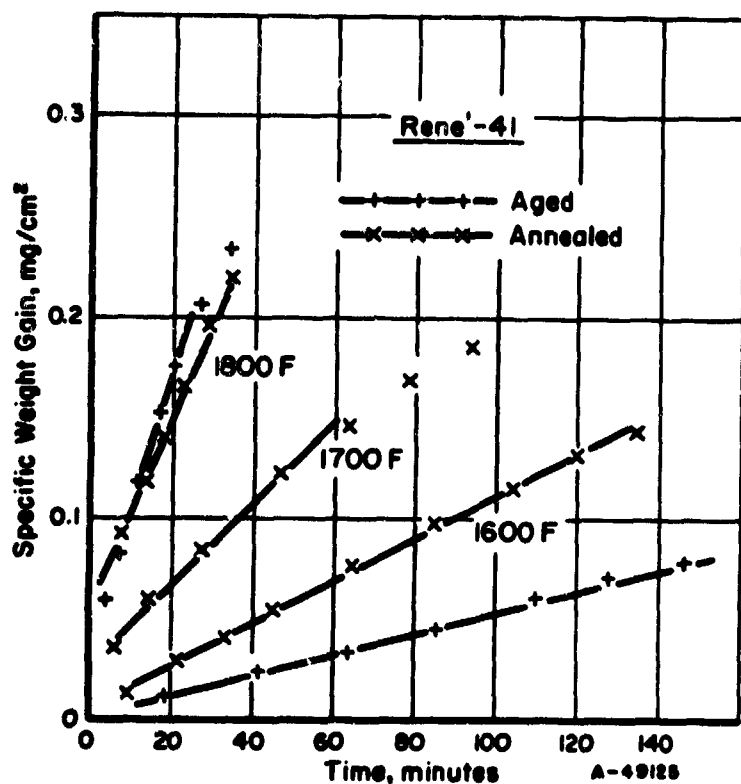


FIGURE 14. LINEAR PLOT OF SPECIFIC WEIGHT GAIN AGAINST TIME FOR A SINGLE HEAT OF RENÉ 41 SHEET<sup>(16)</sup>

Solution annealed 30 min, 2150 F; aged 4 hr, 1600 F.

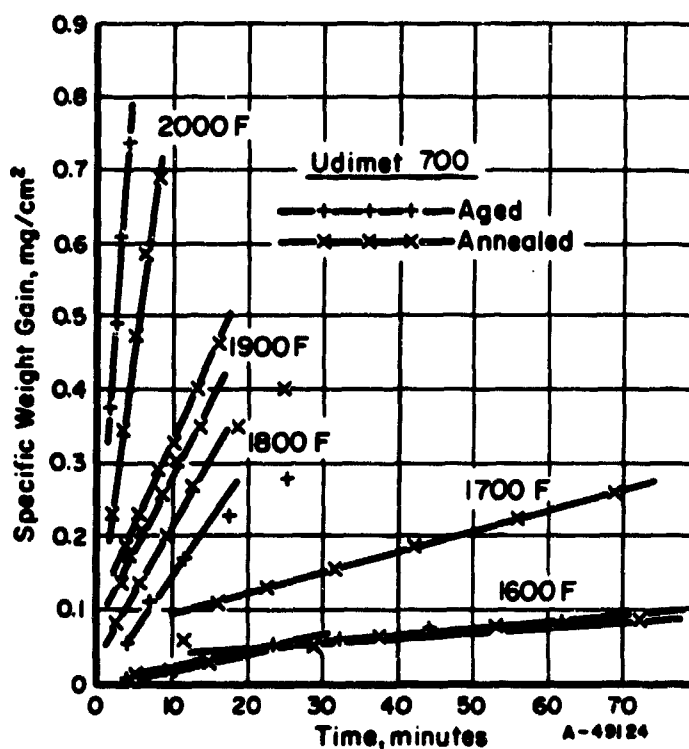


FIGURE 15. LINEAR PLOT OF SPECIFIC WEIGHT GAIN AGAINST TIME FOR A SINGLE HEAT OF CAST UDIMET 700<sup>(16)</sup>

Solution annealed 4 hr, 2150 F; aged 4 hr, 1975 F + 24 hr, 1550 F + 16 hr, 1600 F.

moving air indicate increases in the order of 0.2-0.3 mils at 1200 F, 0.2-0.6 mils at 1500 F, and 0.9 to 1.4 mils at 1800 F.<sup>(17)</sup> Average oxidation (scaling) per side would be half of these values.

Wlodek<sup>(18)</sup> recently reported on the oxidation of Hastelloy X sheet. Both scaling and subscale reactions occurred; the latter are discussed later in this report. The results of continuous weight measurements made on Hastelloy X at tempera-

tures between 1600 and 2200 F are shown in Figure 16. A linear rate curve (slope = 1) is seen for initial oxidation at 1600 F (for over 2000 minutes), but this is ultimately replaced by a parabolic rate (slope = 1/2). The same behavior occurs at 1800 F, but the linear rate persists for only 200 minutes. The results shown in Figure 16 are for a single heat; a second heat showed good duplication of these results at 2000 and 2200 F, but had over 100% greater parabolic rate constant at 1800 F.

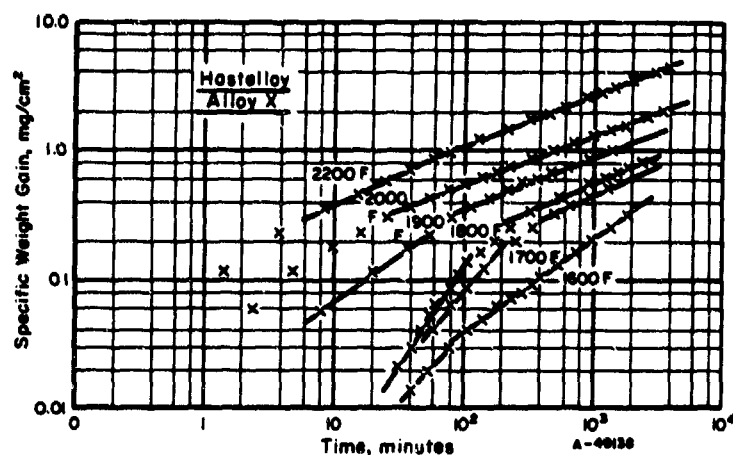


FIGURE 16. LOGARITHMIC PLOT OF SPECIFIC WEIGHT GAIN AGAINST TIME FOR A SINGLE HEAT OF HASTELLOY X(18)

Oxidation of thoriated-nickel (Du Pont's TD-Nickel) was studied by NASA(19), and the results for uncoated specimens are summarized in Figure 17. Note that the oxidation rate for René 41, included in Figure 17 by the NASA workers, shows a considerably higher weight gain at 1800 F, and slightly less at 2000 F, than reported by Wlodek(16). This serves to illustrate the general difficulties in comparing oxidation data.

Oxidation resistance of TRW 1900, a new creep-resistant precision casting alloy, is de-

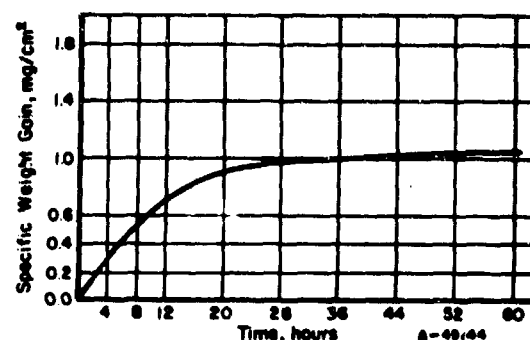


FIGURE 18. OXIDATION RESULTS FOR TRW 1900 OBTAINED AT 2000 F BY WEIGHT GAIN METHODS(20)

scribed in a brochure published by the producer.(20) Service temperatures up to 2150 F are recommended, based on oxidation rates. Weight gain determinations, which imply a uniform scaling attack, are presented in Figure 18 for 2000 F exposure.

Some interesting data on the effect of various elements on the oxidation resistance of a complex nickel-cobalt base alloy were provided by Austin in 1936.(21) The base alloy was K42B

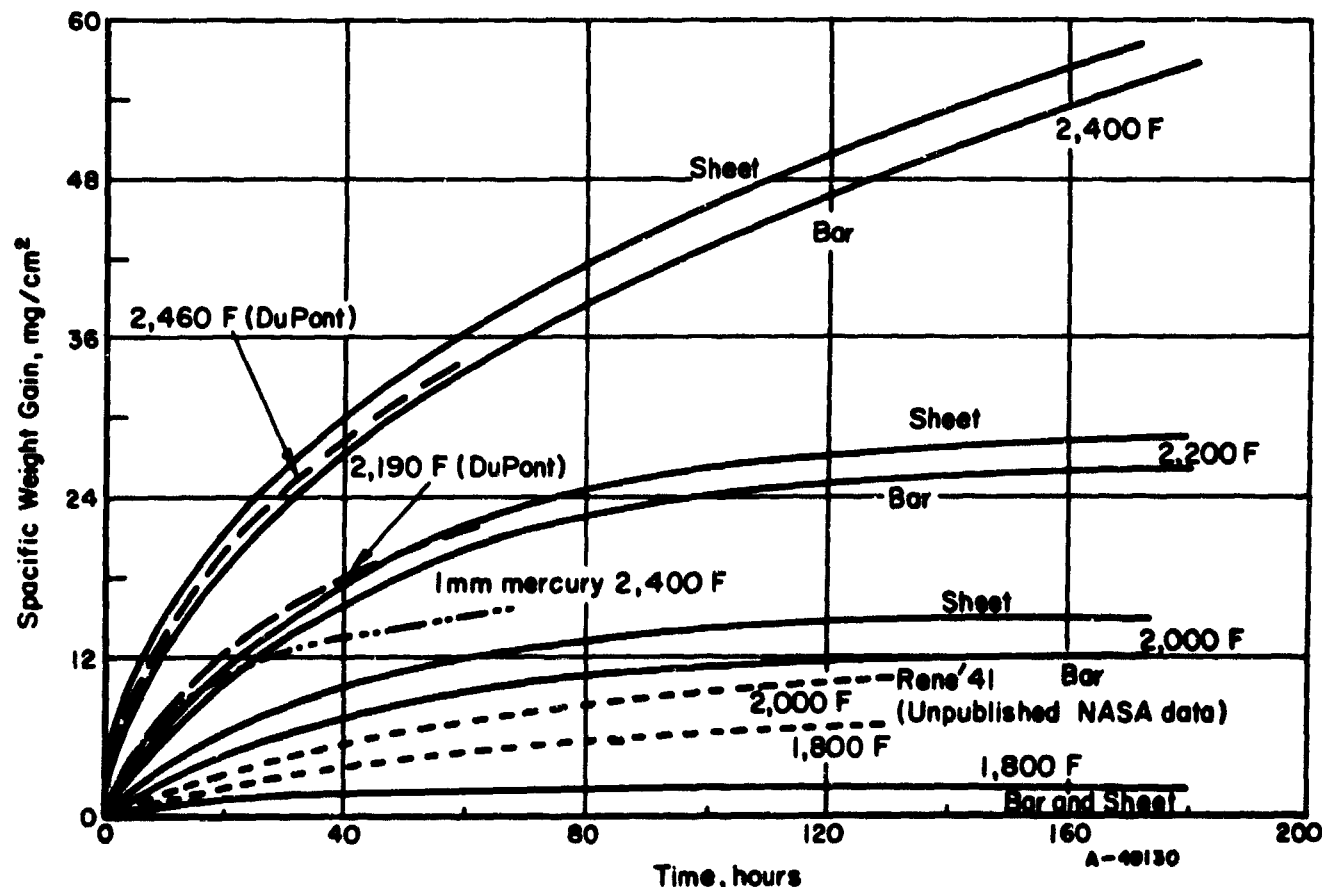


FIGURE 17. LINEAR PLOT OF SPECIFIC WEIGHT GAIN AGAINST TIME FOR THORIATED NICKEL(19)

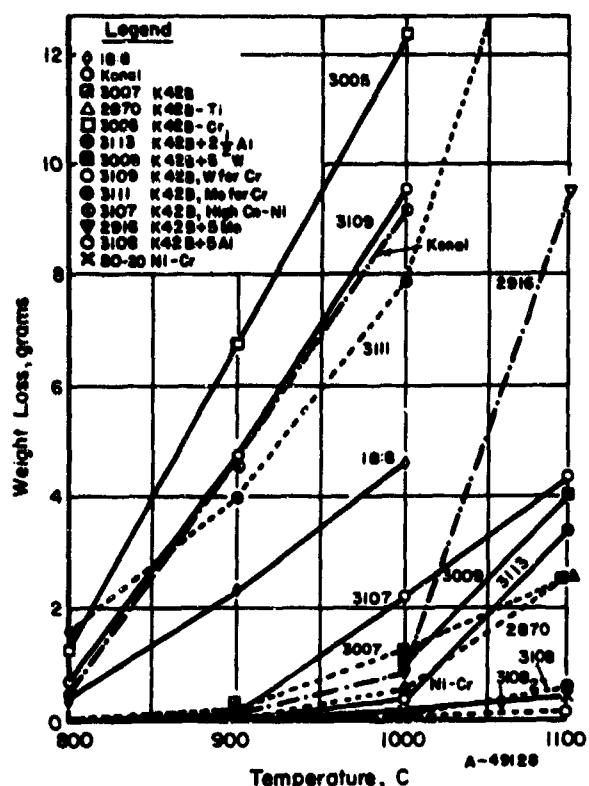


FIGURE 19. EFFECT OF TEMPERATURE ON K42B AND MODIFICATIONS WITH STAINLESS 18-8 AND NICHROME FOR COMPARISON(21)

The data indicate total loss in weight after 400 hours treatment. Specimen size constant, 5/32 inch x 7/8 inch x 3 inches.

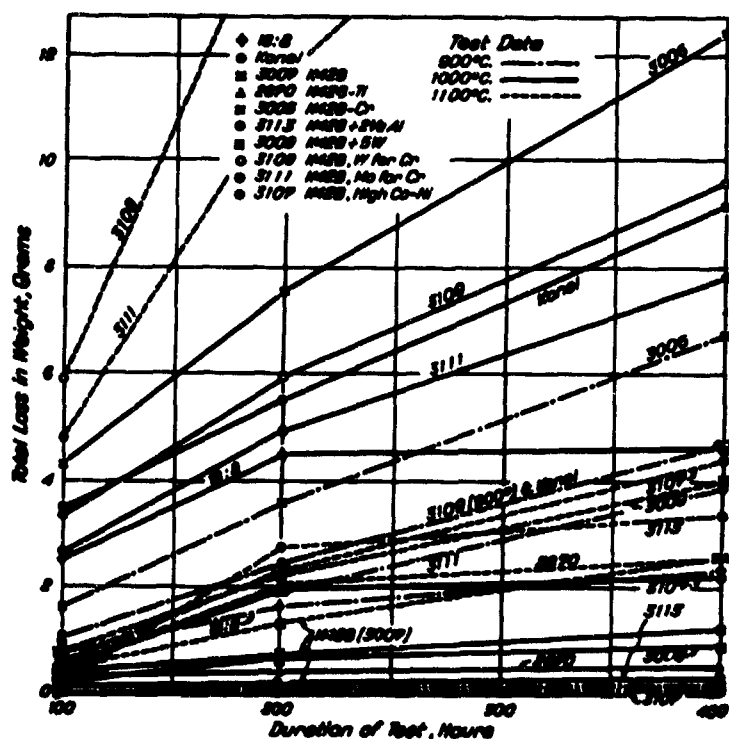


FIGURE 21. EFFECT OF TIME ON PROGRESS OF OXIDATION OF MODIFIED K42B ALLOYS AS REVEALED BY TOTAL WEIGHT LOSS FOR 100, 200, AND 400 HOURS(21)

Data for 900, 1000, and 1100 degrees centigrade are included. Specimen size constant, 5/32 inch x 7/8 inch x 3 inches.

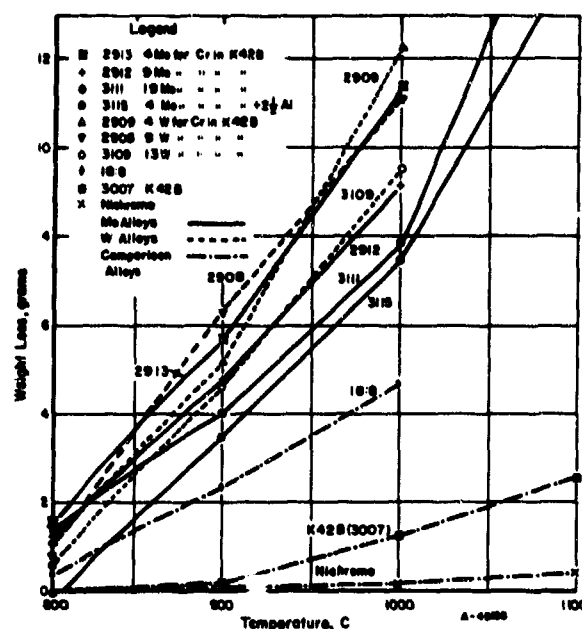


FIGURE 20. COMPARISON OF TEMPERATURE EFFECT BETWEEN K42B TYPE ALLOYS MODIFIED WITH MOLYBDENUM AND WITH TUNGSTEN(21)

Total weight loss after 400 hours treatment recorded. Specimen size constant, 5/32 inch x 7/8 inch x 3 inches.

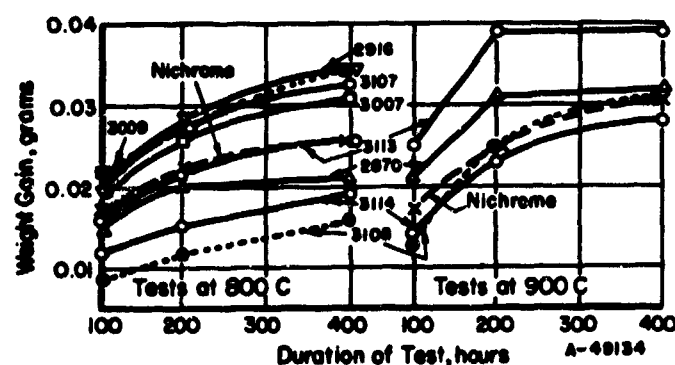


FIGURE 22. COMPARISON OF TIME AND TEMPERATURE EFFECT FOR NICKEL-COBALT-IRON ALLOYS SHOWING HIGH RESISTANCE TO ATMOSPHERIC CORROSION(21)

Specimen size constant, 5/32 inch x 7/8 inch x 3 inches.

containing 45Ni, 25Co, 7.5Fe, 20Cr, 2.5Ti. These data are shown in Figures 19 through 22 and Table 3. Additions of aluminum definitely increase the oxidation resistance lowered by additions of molybdenum (Alloys 2913 and 3115). The effect of titanium can be judged by comparison of Alloys 3007 (normal K42B) and 2870 (K42B minus its normal titanium content), which generally indicates a detrimental effect due to titanium, but not at all times and temperatures of the test.

Freche and Waters(22) reported the oxidation rate at 1900 F of a new nickel-base superalloy, TaZ8



TABLE 3. SUMMARY OF DATA FOR OXIDATION TESTS INCLUDING CHEMICAL ANALYSIS AND MERIT NUMBER OF ALL THE METALS AND ALLOYS SUBJECTED TO TEST<sup>(21)</sup>

Alloy	Chemical Composition				Tests at 800 C			Tests at 900 C			Tests at 1000 C			Tests at 1100 C		Alloy
	Ni	Co	Fe	Ti	Merit No.	Scale(s)	Weight Change	Merit No.	Scale	Weight Change	Merit No.	Scale	Weight Change	Merit No.	Weight Change	
3108	23	47	7.5	2.5	20	Cr 5 Al	1	c.a.	+0.015	2	c.a.	+0.031	2	c.a.	-0.016	3108
3114	46	25	7.5	2.5	19	Cr 5 Al	2	c.a.	+0.019	1	c.a.	+0.028	3	c.a.	-0.061	3114
2870	48	25	7.0	...	20	Cr	3	c.a.	+0.021	4	c.a.	+0.032	6	c.a.	-0.518	2870
NiCr IV	80	...	...	...	20	Cr	4	c.a.	+0.025	2	c.a.	+0.031	4	c.a.	-0.11	NiCr IV
3113	46	25	7.5	2.5	19	Cr 2.5 Al	5	c.a.	+0.025	5	c.a.	+0.039	5	c.a.	-0.320	3113
3007 (K42B)	45	25	7.5	2.5	20	Cr	6	c.a.	+0.030	12	c.a.	-0.112	9	c.a.	-1.241	3007 (K42B)
3107	23	47	7.5	2.5	20	Cr	7	c.a.	+0.032	11	c.a.	-0.071	10	c.a.	-2.241	3107
2916	44	24	7.5	2.5	17	Cr 5 Mo	8	c.a.	+0.034	9	c.a.	-0.047	7	c.a.	-0.881	2916
3009	44	24	7.5	2.5	17	Cr 5 W	9	c.a.	+0.034	10	...	-0.065	8	60 s.	-0.906	3009
3006	47	30	7.5	2.5	13	Cr	10	c.a.	+0.051	8	...	-0.033	11	c.a.	-2.611	3006
2868	26	54	7.5	2.5	10	Cr	11	c.a.	+0.098	15	90 s.	-3.20	13	c.a.	-4.457	2868
Nickel	...	...	...	...	...	...	12	c.a.	+0.171	7	c.a.	+0.511	1	c.a.	+1.034	Nickel
2920	77	20	...	...	3	Si	13	c.a.	+0.194	6	c.a.	+0.058	12	80 s.	-3.994	2920
2915	30	50	10.0	...	8	Cr 2 Va	14	c.a.	+0.240	28	c.s.	-9.35	28	c.s.	-18.33	2915
3115	56	30	7.5	2.5	4	Mo 2.5 Al	15	95 s.	+0.260	16	c.s.	-3.46	16	c.s.	-7.47	3115
18-8	8	...	74.0	...	18	Cr	16	c.s.	-0.342	14	c.s.	-2.324	14	c.s.	-4.637	18-8
Konal	73	17	7.5	2.5	...	...	17	50 s.	-0.407	20	c.s.	-4.67	19	c.s.	-9.128	Konal
3004	58	27	10.5	4.5	...	...	18	c.s.	-0.474	18	c.s.	-3.93	18	c.s.	-8.863	3004
3008	15	40	42.5	2.5	...	...	19	c.s.	-0.500	13	50 s.	-1.51	15	90 s.	-5.233	3008
3109	49	26	7.5	2.5	15	W	20	50 s.	-0.614	20	c.s.	-4.67	21	c.s.	-9.537	3109
2908	53	29	7.5	2.5	8	W	21	c.s.	-0.866	26	c.s.	-6.29	23	c.s.	-11.14	2908
K52	40	41	16.0	2.5	...	...	22	c.s.	-0.916	17	c.s.	-3.9	22	c.s.	-11.014	K52
2909	56	30	7.5	2.5	4	W	23	90 s.	-1.090	23	c.s.	-5.11	26	c.s.	-12.29	2909
2912	53	29	7.5	2.5	8	Mo	24	c.s.	-1.117	22	c.s.	-4.73	20	c.s.	-9.17	2912
3005	58	32	7.5	2.5	...	...	25	65 s.	-1.251	27	c.s.	-6.76	27	c.s.	-12.40	3005
2867	27	54	15.0	4.0	...	...	26	70 s.	-1.396	25	c.s.	-6.03	25	c.s.	-11.634	2867
3111	46	25	7.5	2.5	19	Mo	27	c.s.	-1.410	19	c.s.	-3.95	17	c.s.	-7.831	3111
2914	30	58	7.5	2.5	2	Va	28	75 s.	-1.452	29	c.s.	-13.4	29	c.s.	-17.21(b)	2914
2913	56	30	7.5	2.5	4	Mo	29	c.s.	-1.573	24	c.s.	-5.61	24	c.s.	-11.40	2913
Cobalt	...	...	...	...	...	...	30	c.s.	-18.071	30	...	...	30	...	...	Cobalt

(a) c. a. - completely adherent.

c. s. - completely scaled.

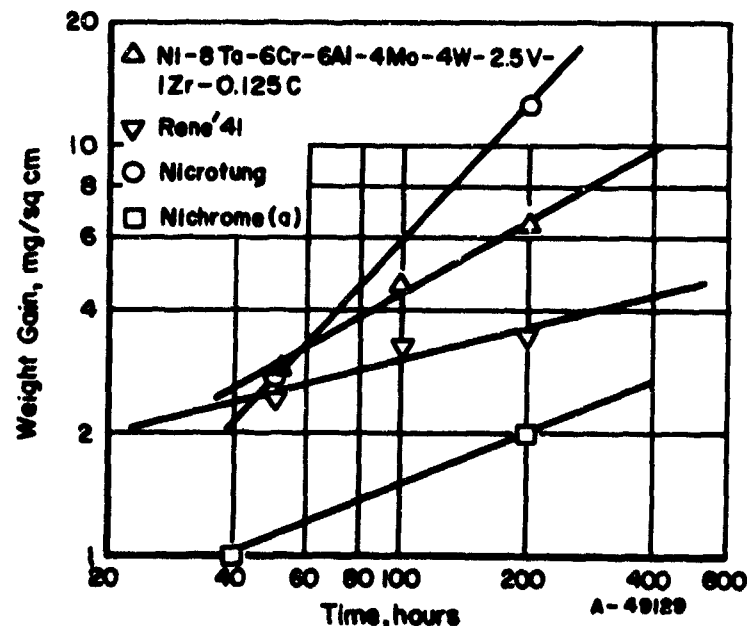
(b) 200 hours.

Specimens size constant, 5/32 inch x 7/8 inch x 3 inches. Values recorded indicate total change in weight in grams after 400 hours.

(Ni-8Ta-6Al-6Cr-4Mo-4W-2.5V-1Zr-0.125C). Figure 23 shows the results, and compares the oxidation rate of the new alloy with the oxidation rate of René 41 and Nicrotung, which were tested simultaneously with the experimental alloy. Data on Nichrome are also included.

The microstructures of the experimental NASA alloy, René 41, and Nicrotung after a 200-hour oxidation test at 1900 F are shown in Figure 24<sup>(22)</sup>. A relatively uniform layer of oxide scale is seen on the surface of the René 41, and partially on the Nicrotung. None is visible on the NASA alloy, but it was reported that the scale probably spalled off during cooling between 800 and 600 F. Between the surface oxide and the unaffected material is a depleted zone which evidently varies in thickness a great deal among the three alloys shown here. In addition, considerable intergranular attack has occurred in the René 41 and Nicrotung.

An interesting study of the oxidation behavior of fine wires was made by Johnson, et al.<sup>(23)</sup> Figure 25 and Table 4 summarize some of their findings. One interesting item is the apparent increase in specific oxidation rate with increase in wire size. More is said about the effects of section size in the section of this report on intergranular oxidation.

FIGURE 23. WEIGHT GAIN PER UNIT AREA AS A FUNCTION OF TIME AT 1900 F FOR SEVERAL NICKEL-BASE ALLOYS<sup>(22)</sup>

(a) From: Barrett, C. A., Evans, E. B., and Baldwin, W. M., Jr., "Thermodynamics and Kinetics of Metals and Alloys - High-Temperature Scaling of Ni-Cr, Fe-Cr, Cu-Cr, and Cu-Mn Alloys", Final Technical Report, March to November, 1955, Case Institute of Technology (December, 1955).

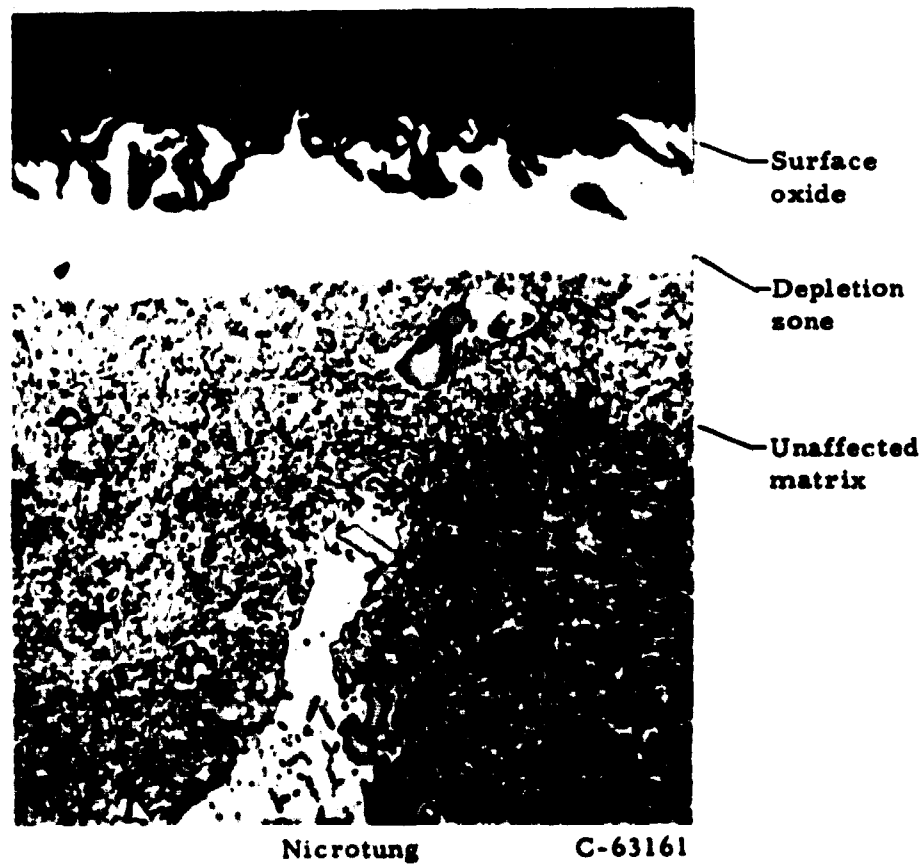
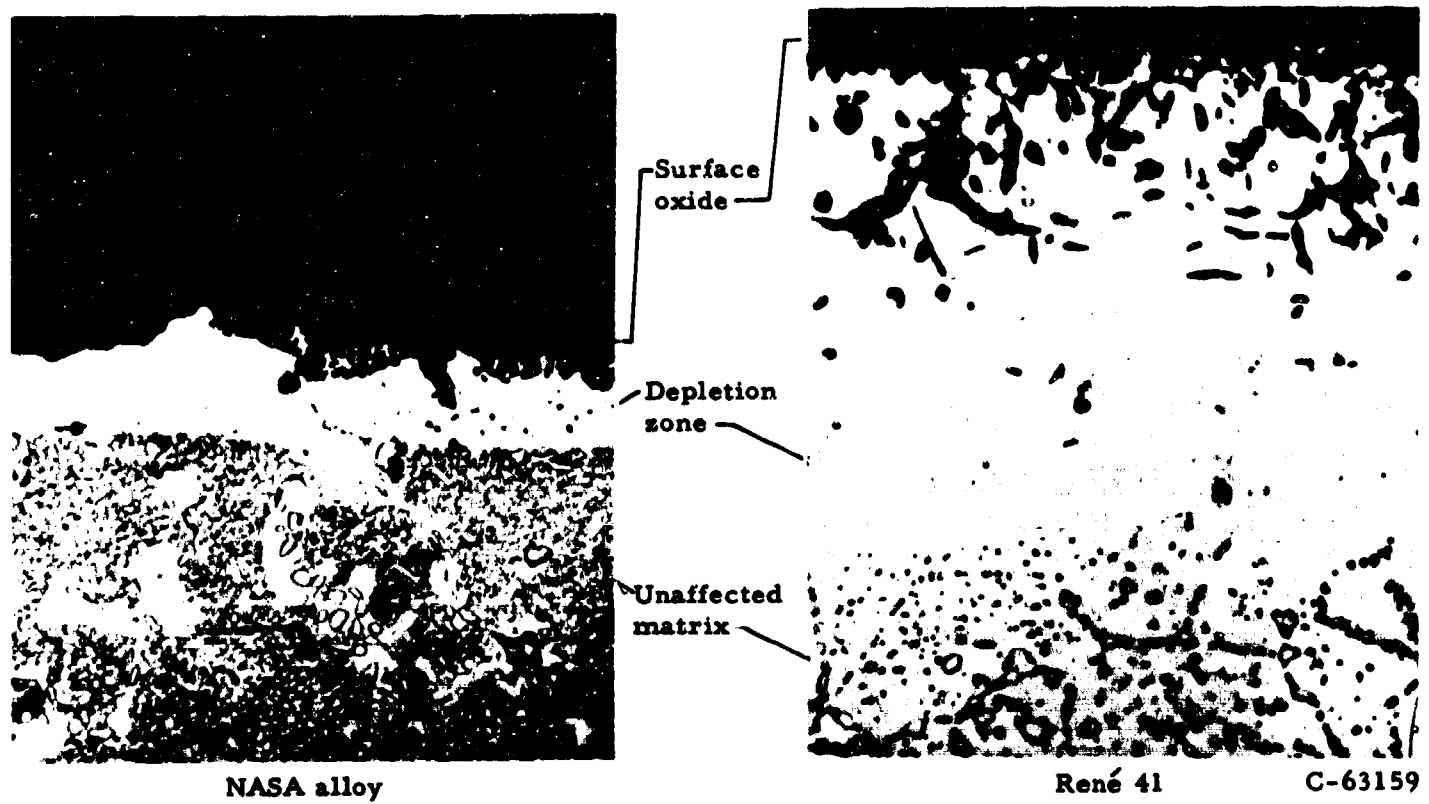


**FIGURE 24. MICROSTRUCTURE OF OXIDATION TEST SPECIMENS IN VICINITY OF EXPOSED SURFACE AFTER 200 HOURS EXPOSURE AT 1900 F**

750 X. The photographs have been reduced approximately 20 per cent in printing.

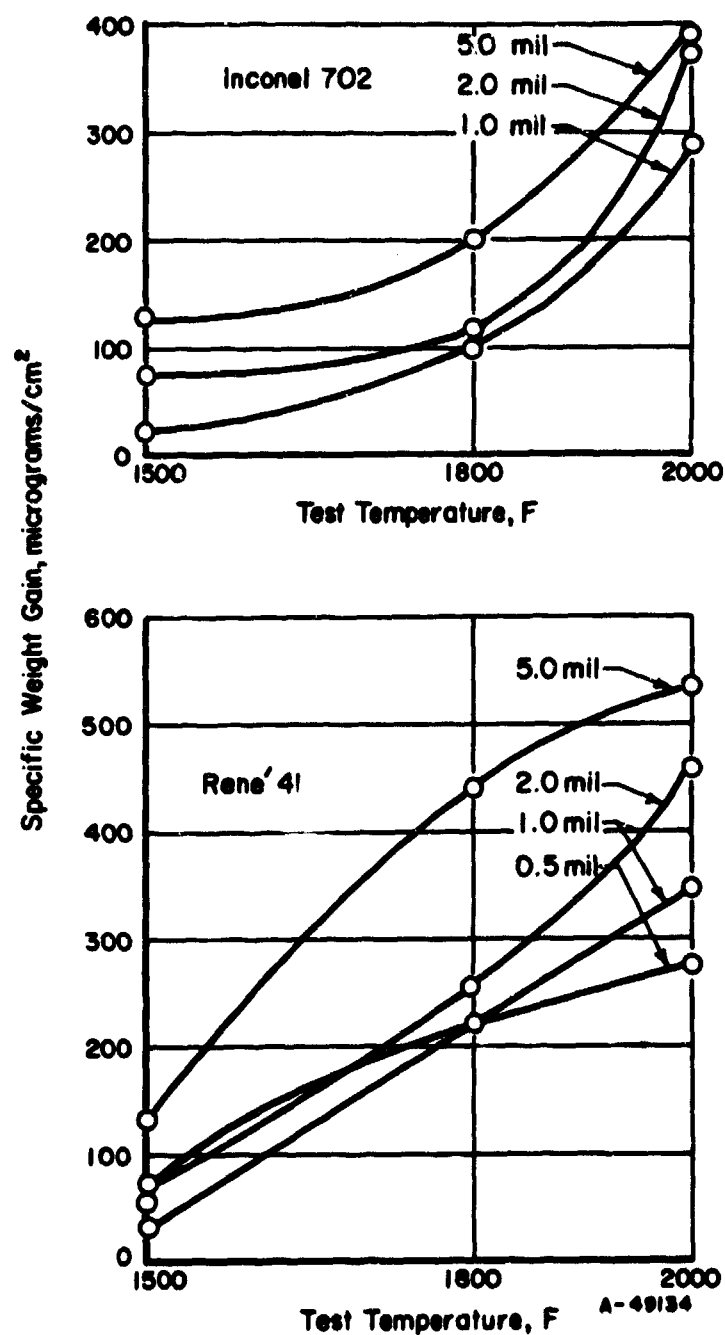


FIGURE 25. OXIDATION OF FINE WIRE OF VARIOUS DIAMETERS AFTER 10 MINUTES EXPOSURE TO AIR

After Johnson, et al. (23)

Data on the oxidation resistance of several cobalt-base alloys are given in Figures 26 through 30, and in Table 5. Some early work by Ecker and Huffman<sup>(24)</sup> is shown in Figures 26, 27, and 28 for Alloys S-816, Haynes Stellite Alloy 21, and Haynes Stellite Alloy 31, respectively. Data from Eberle, et al.,<sup>(25)</sup> are superimposed on Figure 27, and show good correlation with the data of Ecker and Huffman. In all cases, the results are reported in terms of weight gain.

Weight gain data for L-605 and X-40 (same as Haynes Stellite Alloy 31) were reported recently by Wlodek.<sup>(26)</sup> Figures 31 and 32 show the results. In the case of X-40, very erratic behavior was

13

TABLE 4. PARABOLIC RATE LAW CONSTANTS,  $k$ , FOR OXIDATION OF FINE WIRES<sup>(23)</sup>

Wire Diameter, mils	$k \times 10^{11}$		
	René 41	Elgiloy	Inconel 702
<u>At 2000 F</u>			
0.5	13	2.1	--
1.0	21	10	14
2.0	37	11	23
5.0	45	24	27
<u>At 1800 F</u>			
0.5	7.5	0.91	--
1.0	9.2	3.0	1.7
2.0	11	6.0	2.0
5.0	26	13	6.7
<u>At 1500 F</u>			
0.5	0.84	0.28	--
1.0	0.16	3.7	0.1
2.0	0.84	3.1	1.2
5.0	3.1	1.8	2.8

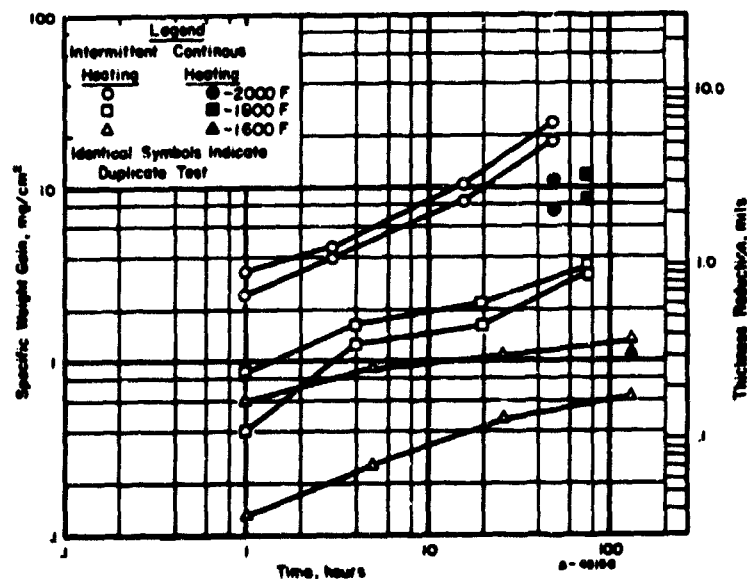


FIGURE 26. RATE OF OXIDATION OF S-816 SHEET<sup>(24)</sup>

noted, and further characterization of the oxidation rate was not possible. Note also that the magnitude of the weight gain is much less than reported by Ecker and Huffman.<sup>(24)</sup> At temperatures of 1600 F and below, L-605 also showed erratic behavior. However, after 1000 minutes

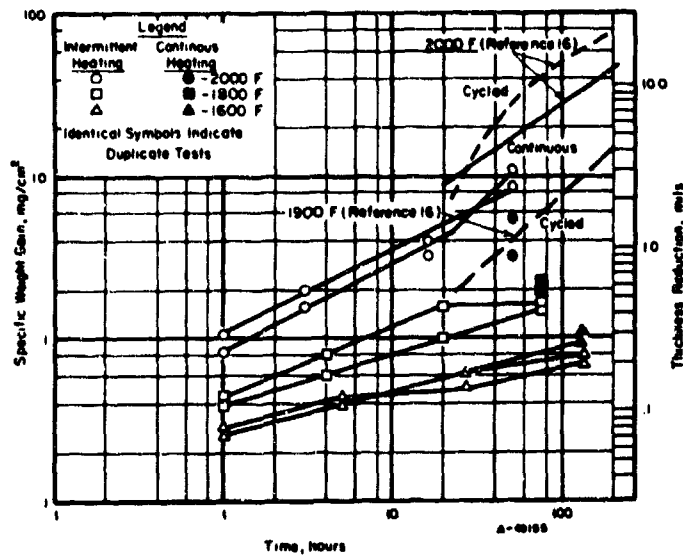


FIGURE 27. RATE OF OXIDATION OF HAYNES STELLITE 21 (24, 25)

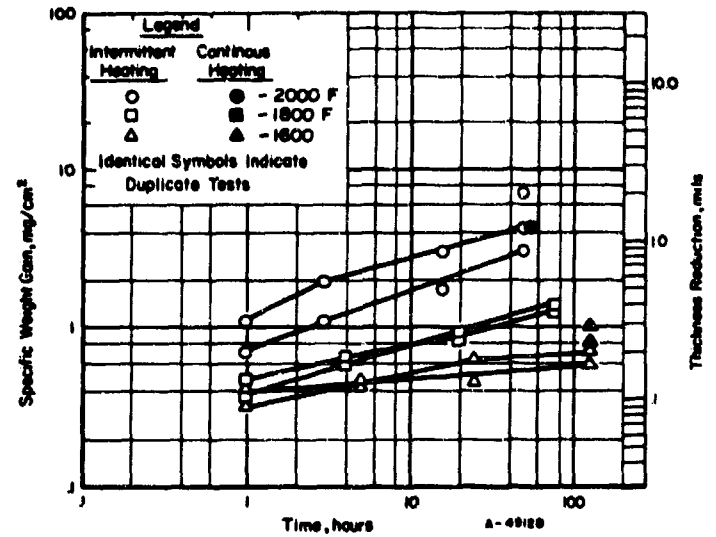


FIGURE 28. RATE OF OXIDATION OF HAYNES STELLITE 31 (24)

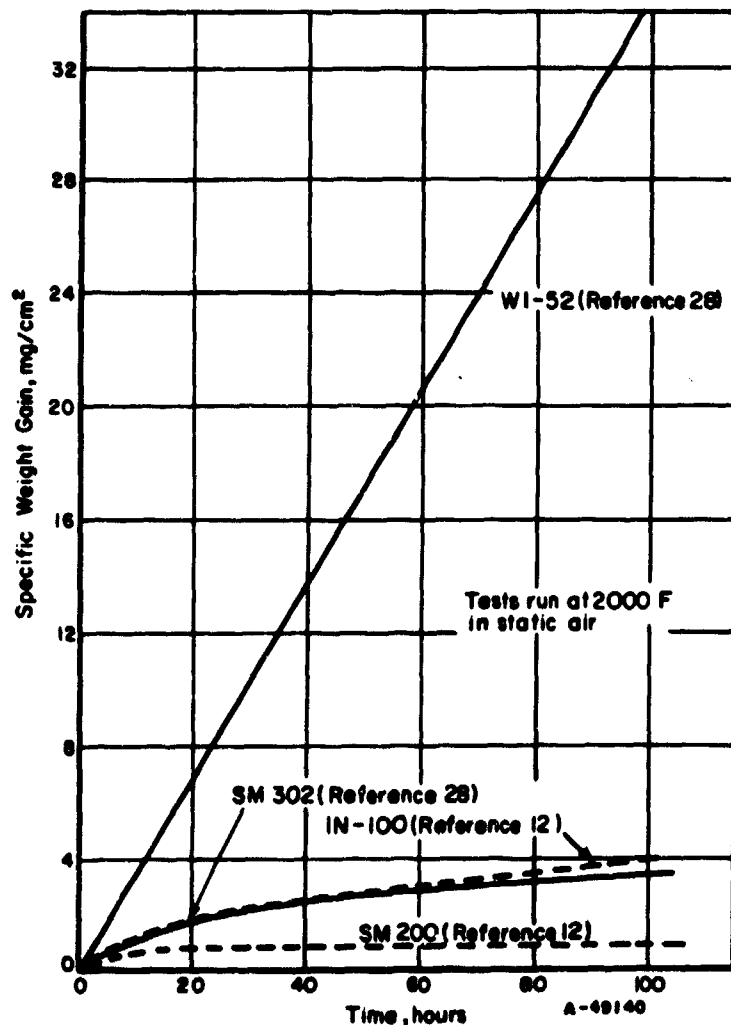


FIGURE 29. OXIDATION RESISTANCE OF TWO COBALT-BASE SUPERALLOYS COMPARED WITH THAT OF TWO NEW NICKEL-BASE SUPERALLOYS (12, 28)

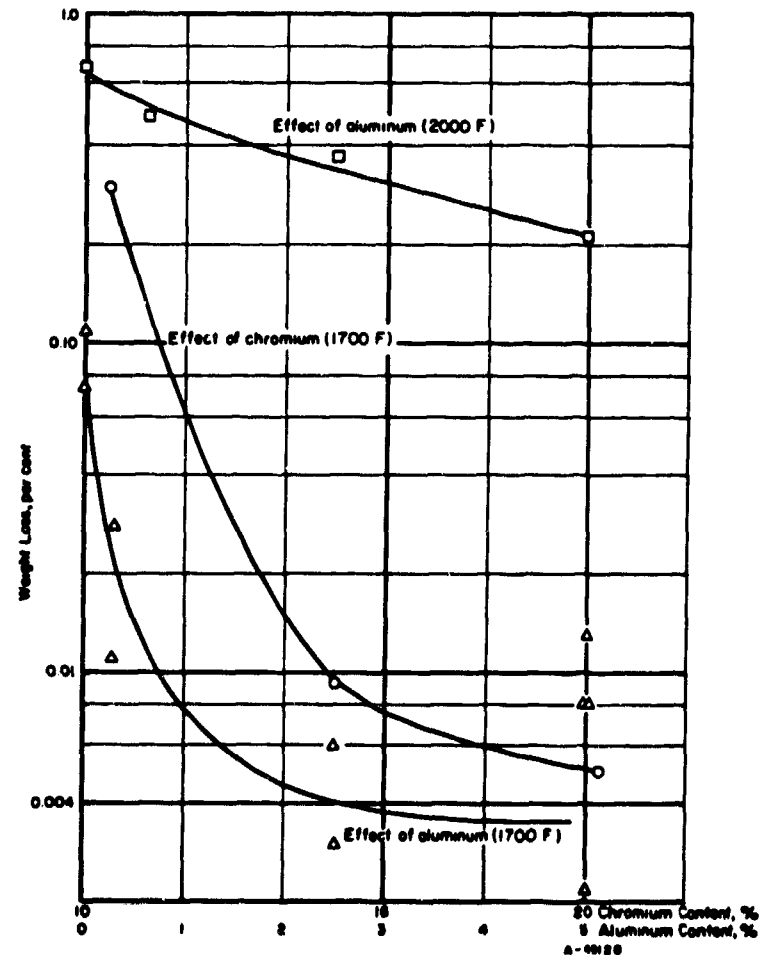


FIGURE 30. EFFECT OF ALUMINUM AND CHROMIUM CONTENT ON THE OXIDATION RATE OF AF-94 MODIFICATIONS (28)

Based on 100-hr tests made in still air at 1700 and 2000 F. Specimen size, 0.5 in. diam x 0.5 in. long.

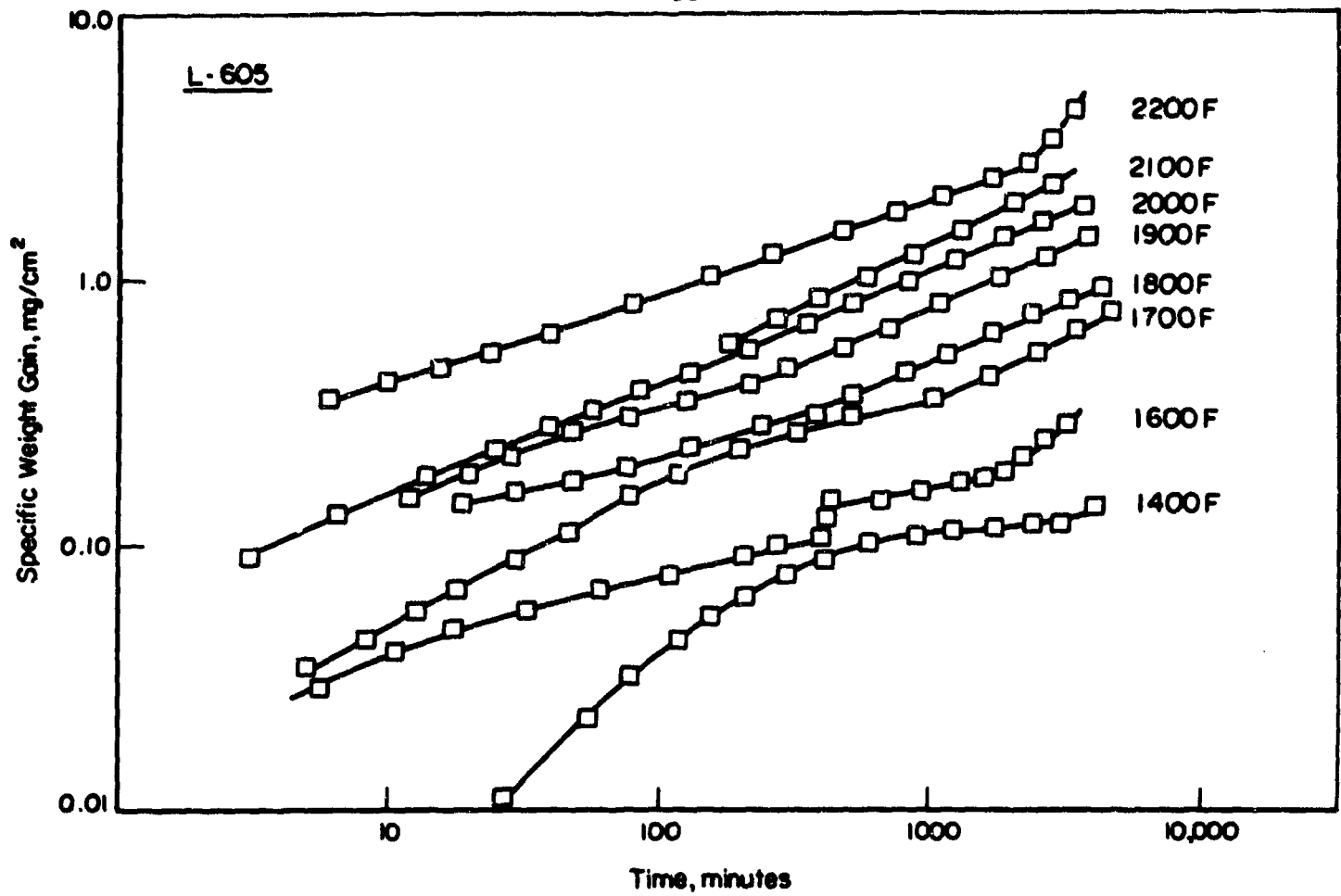


FIGURE 31. LOG-LOG PLOT OF WEIGHT GAIN DATA FOR L-605(26)

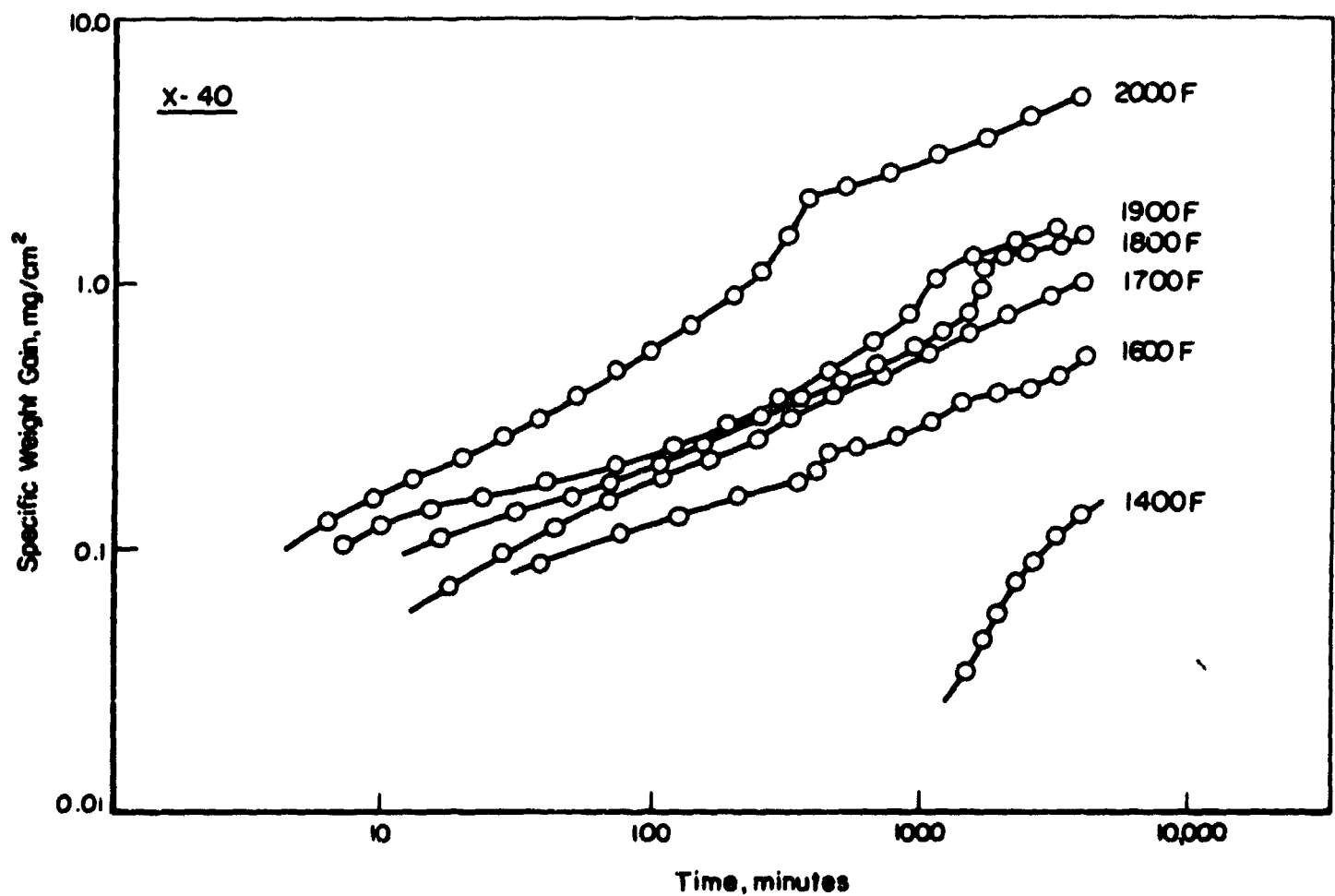


FIGURE 32. LOG-LOG PLOT OF WEIGHT GAIN DATA FOR X-40(26)

at 1700 F or after 10 to 100 minutes at higher temperatures a reproducible parabolic rate was observed. The erratic behavior of L-605 was ascribed mainly to extremely heterogeneous scale distribution. Some areas of specimens oxidized at 1400 F, for example, were virtually free of oxide. X-40 also oxidized heterogeneously, but the cause seems to have been preferential oxidation in areas containing high-tungsten  $M_6C$ -type carbide phases, as well as other variations in chemical composition.

The main scale product on L-605 was found by Wlodek to be a spinel of the form  $CoCr_2O_4$ . During parabolic oxidation, smaller amounts of  $Cr_2O_3$  and  $CoO$  were found. At a temperature of 2200 F catastrophic attack seems to have been associated with the formation of a low-melting scale of  $CoW_4$ ,  $Co_3O_4$ ,  $CoO$ , and  $CoCr_2O_4$ . Generally, the oxidation products found on X-40 were the same as for L-605, though a much smaller amount of catastrophic oxidation hindered positive identification of  $CoW_4$ .

Measurement of the increase in total thickness of L-605 sheet indicates 0.1-0.3 mil at 1200 F, 0.2-0.5 mil at 1500 F, and 0.7-1.2 mils at 1800 F, all for 50 hours.(17)

Data for the wrought alloy J-1570 as reported by Dempsey(27) are shown in Table 5. In these tests, the specimens were exposed for 16 hours at 2000 and 2200 F, descaled, and then exposed for another 16 hours.

TABLE 5. CORROSION BEHAVIOR OF ALLOY J-1570(27)

Specimen	Temperature, F	Weight Loss, g	
		During First 16 Hours	During Second 16 Hours
1	2000	0.1199	0.2418
2	2000	0.1041	--
3	2200	0.4527	1.0515

Note: Specimen size was 1/4 in. x 1/4 in. x 3/4 in.

Information on the oxidation resistance of SM302 and WI-52 cobalt-base superalloys is shown in Figure 29.(28)\* Data previously shown for nickel-base alloys IN-100 and SM200 are included for comparison purposes, as the tests apparently were conducted under identical conditions.

\*Further information on the oxidation characteristics of SM302 was recently published by E. J. Felten and R. A. Gregg in Transactions of the American Society for Metals, 57, 804-822 (1964). In addition, NASA investigators J. C. Freche, R. L. Ashbrook, and G. D. Sandrock recently published information on the oxidation resistance of cobalt-tungsten alloys (Trans. ASME, Series B, February, 1965, pp 9-20).

MacFarlane, Pitler, and Reynolds (Figure 30) showed that aluminum and chromium are beneficial to the oxidation resistance of a cobalt-base alloy.(29) The alloy used as a basis was AF-94, a cobalt-base alloy containing normally 0.12C, 15Cr, 10Ni, 5Mo, 10W, 1(Cb + Ta). The oxidized specimens were descaled in a hot caustic solution, and thus the results are shown in terms of weight loss. The loss is reported as a percentage, but the data can be considered within their own framework as the specimen size was held constant throughout (0.500 in. in diameter x 0.500 in. long).

#### INTERGRANULAR OXIDATION

A comparison of the results of oxidation experiments using the weight-gain or weight-loss method may not indicate the full extent of oxidation change. Superalloys, particularly the precipitation-hardenable nickel-base family, are susceptible to intergranular oxide penetration. While this type of attack may have little effect on the strength of articles of large cross section, it can be a serious problem in the case of thin sheet, foil, and fine wire. While it is possible for the general surface oxidation to be practically nil and of little importance in these thin sections, even a small amount of intergranular penetration may lead to premature failure. For example, penetration of 2 mils from each side of a 15-mil sheet would reduce its load bearing cross section by about 27 per cent. Penetrations of this order, e.g., 1-2 mils, are not unusual for the superalloys. Fortunately, intergranular penetration takes place only at relatively high temperatures.

Time-temperature-penetration curves have been obtained for René 41, as shown in Figure 33.(30)

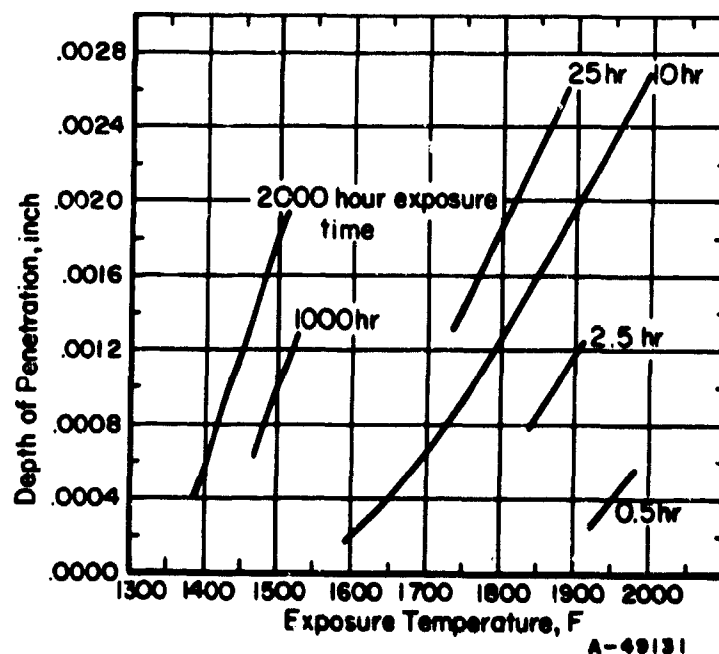


FIGURE 33. DEPTH OF OXIDATION VERSUS TEMPERATURE FOR RENÉ 41(30)

The curves show the depth of intergranular oxidation. The depth of uniform oxidation is negligible.

In this figure, it can readily be seen that intergranular penetration increases greatly with increasing time and temperature. For example, the time for 1-mil penetration (2 mils total, 1 mil from each side) to occur, changes from about 1000 hours at 1500 F, to 10 hours at 1750 F, 2.5 hours at 1850 F, and about 0.8 hour at 2000 F.

Similar, though not identical, results were obtained by Childers and Koriagin<sup>(31)</sup>, as shown in Figure 34. These results are for oxidation at sea level, and somewhat less severe attack may occur at reentry altitudes, according to preliminary data presented in Table 6. On the other hand, the effects of dynamic pressure and velocity were not evaluated. Consequently, the data obtained cannot be used to determine the extent of attack during actual reentry conditions.

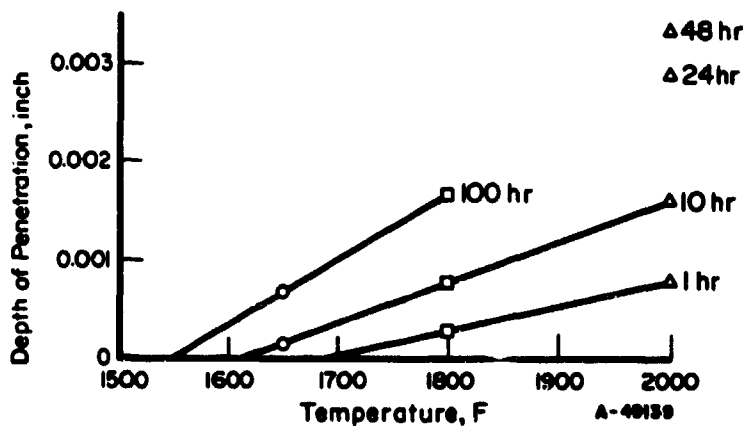


FIGURE 34. EFFECT OF TIME AND TEMPERATURE ON OXIDE PENETRATION OF RENÉ 41 IN STILL AIR<sup>(31)</sup>

TABLE 6. EFFECT OF AMBIENT PRESSURE ON OXIDATION OF RENÉ 41<sup>(31)</sup>

Exposure Temperature, F	Time of Exposure	Ambient Pressure, mm Hg	Depth of Penetration, in.
2000	100 min.	Sea Level	0.00084
2000	100 min.	0.090	0.00080
2000	1800 hr.	$10^{-4}$	None

Information on oxide penetration is of great importance now that increasing use is made of thin sheet for structural applications at high temperatures. It is also important in the heat treatment of sheet. Temperatures of 1950 to 2150 F are regularly used in the solution treatment prior to aging. Thus, finished sheet may be susceptible to penetration during heat treatment. Aging temperatures are too low to be of importance to the problem at hand.

Intergranular oxide penetration affects not only the tensile and stress-rupture properties by reducing the effective cross section, but it also can be expected to be detrimental to the fatigue strength because the "tongue" of corrosion will act as a notch.<sup>(32)</sup>

Figures 35 and 36, from Simenz<sup>(33)</sup>, show the intergranular attack on several nickel- and cobalt-base alloys. Figure 35 gives the results of a 1-hour exposure at various temperatures from 1600 to 2200 F. Figure 36 shows the results of ten 1-hour cyclic exposures at these same temperatures. The data are for a single side and would be doubled if attack was present on both sides. It is interesting to note that the solid-solution-hardened Hastelloy X gives lower oxide penetration than the precipitation-hardened nickel-base alloys at all temperatures during the cyclic test.

Figure 37 gives the oxide penetration after 100 hours in slow-moving air for three International Nickel Company alloys and AMS 5537 (L-605 cobalt-base alloy).<sup>(34)</sup> In these tests, the aluminum-bearing alloy, Inconel 702, showed less intergranular penetration than did the titanium-bearing alloy, Inconel X.

Ignatov stated that additions of 4 per cent aluminum to 80-nickel-20-chromium alloys prevents intergranular oxidation. Additions of titanium on the other hand increase the intergranular oxidation.<sup>(5)</sup> The difference lies in the structure of the oxides formed and the fact that  $\text{Ni}_3\text{Ti}$  lies in the grain boundaries. Aluminum forms the dense, closely packed  $\text{Al}_2\text{O}_3$  structure, whereas titanium

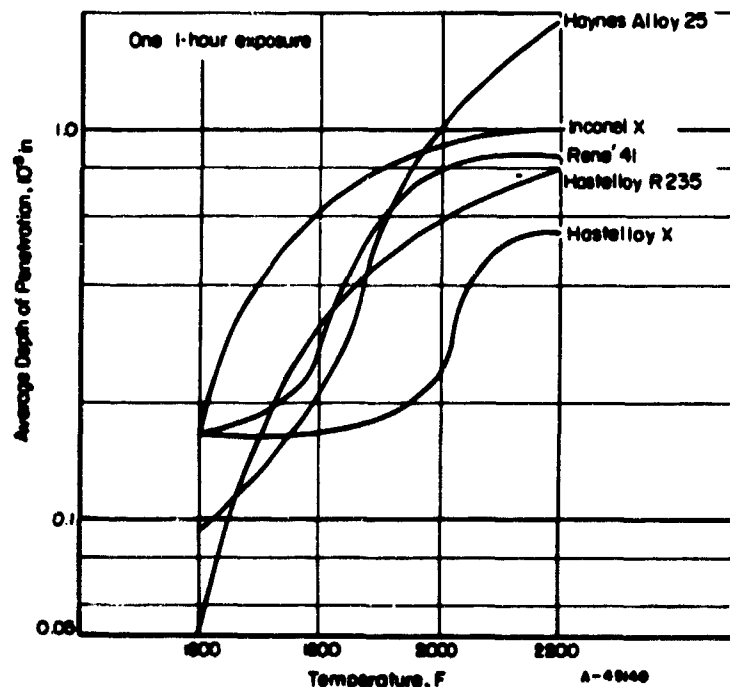


FIGURE 35. DEPTH OF ATTACK AS A FUNCTION OF TEMPERATURE FOR VARIOUS ALLOYS<sup>(33)</sup>

forms the defect (anion deficient) structure of rutile,  $\text{TiO}_2$ . Oxidation of nickel-chromium alloys normally proceeds by diffusion of the metallic ions through the oxide to the outer surface, where they combine with oxygen. Accordingly, diffusion of metallic ions to the oxide-metal interface is the rate-controlling process. However, the defect structure of rutile permits a greater proportion of oxygen diffusion inward to the interface, resulting in a higher rate of oxidation at the oxide-metal interface in titanium-bearing alloys than in aluminum-bearing ones.

Dukes, et al., studied the oxidation behavior of a nickel-base alloy, Inconel 702, and a cobalt-base alloy, Haynes Alloy 25 (L-605).<sup>(35)</sup> The results of these studies are given in Figures 38 and 39.<sup>(35)</sup> Figure 38 illustrates the excellent oxidation resistance of Inconel 702.

When wires and sheet of 6-mil thickness are intergranularly attacked on all surfaces to a depth of 2 mils, the sheet retains one-third its original effective cross-sectional area, whereas the wire retains only one-ninth. Figures 40 and 41 illustrate the effect of oxidation on the room-temperature strength properties of René 41 and Inconel 702 wire, respectively, after exposure in static air for 5 minutes at various elevated temperatures.<sup>(23)</sup> These curves show that the effective cross section of fine wires held at high

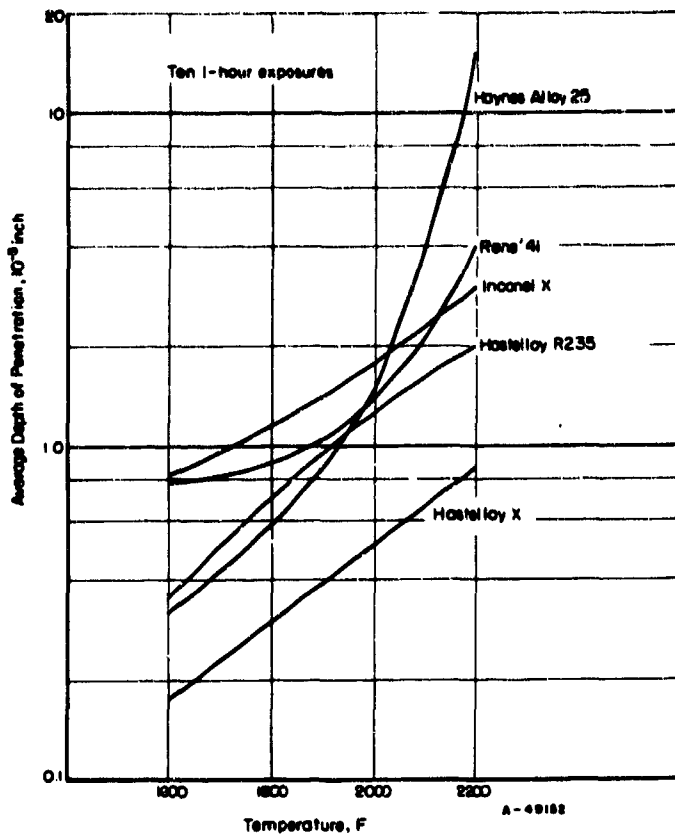


FIGURE 36. DEPTH OF ATTACK OF VARIOUS ALLOYS CYCLED TEN TIMES TO THE INDICATED TEMPERATURES<sup>(33)</sup>

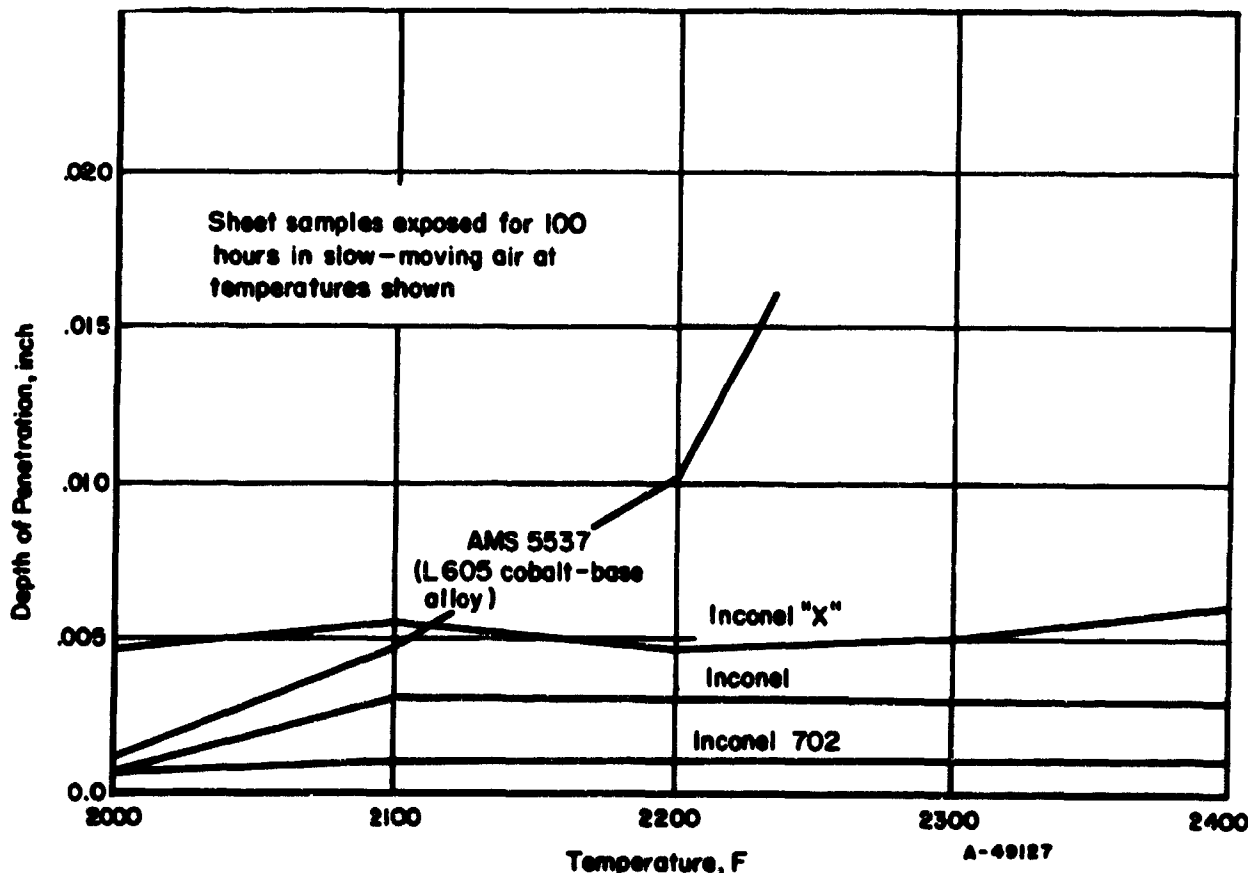


FIGURE 37. DEPTH OF PENETRATION VERSUS TEMPERATURE FOR SEVERAL NICKEL- AND COBALT-BASE ALLOYS<sup>(27)</sup>



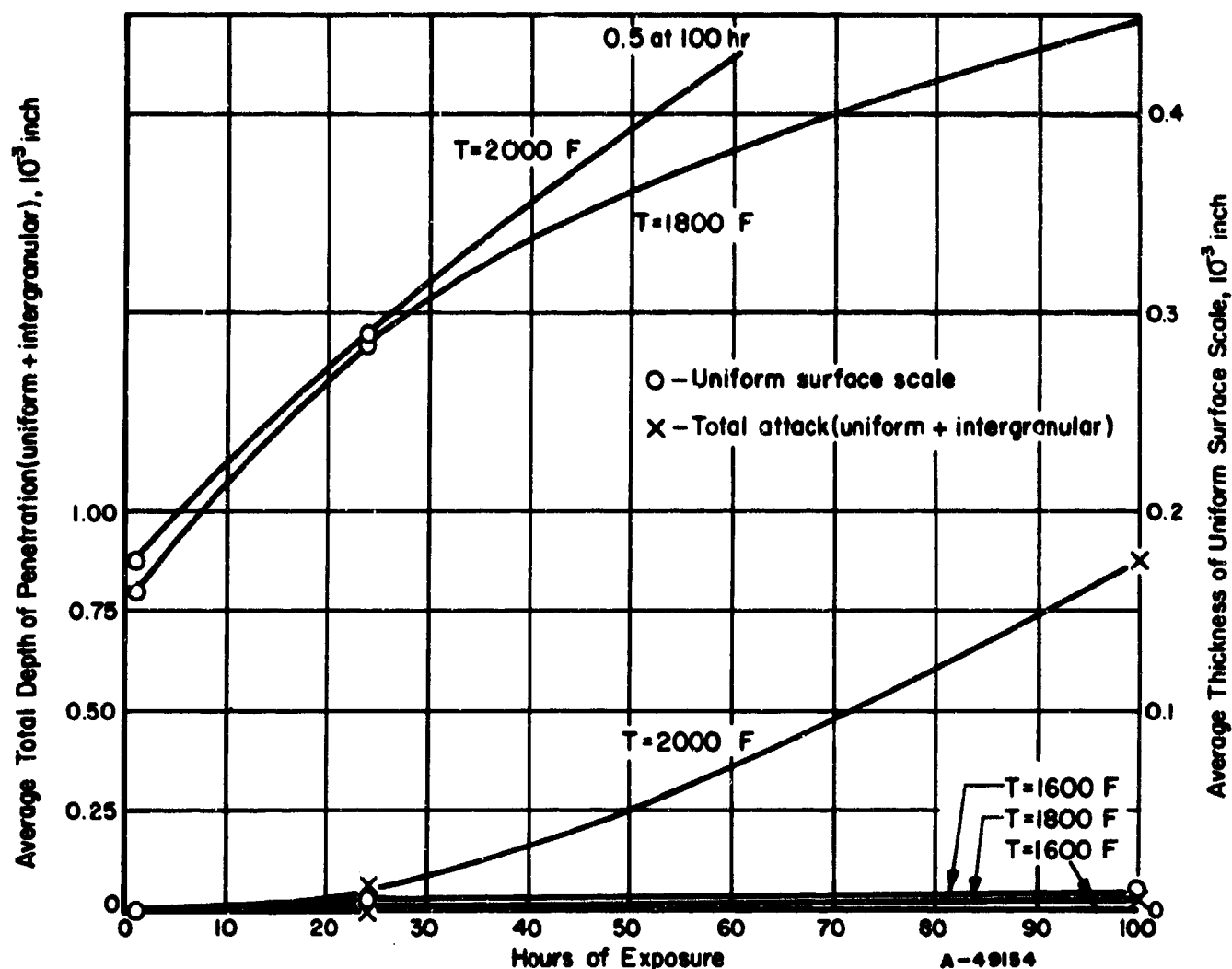


FIGURE 38. OXIDATION BEHAVIOR OF INCONEL 702 SHEET EXPOSED TO AIR AT ELEVATED TEMPERATURES<sup>(35)</sup>

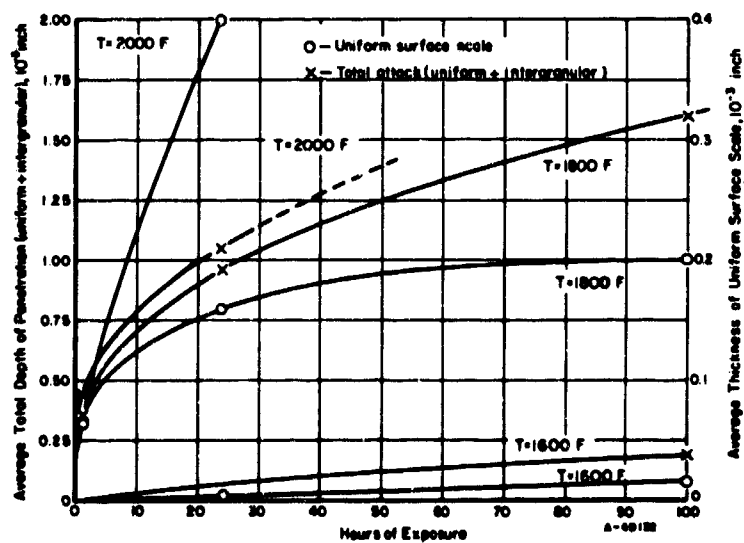


FIGURE 39. OXIDATION BEHAVIOR OF HAYNES ALLOY 25 SHEET EXPOSED TO AIR AT ELEVATED TEMPERATURES<sup>(35)</sup>

temperatures can be entirely consumed by oxidation. Table 7 shows the effect of oxide penetration on the short-time tensile strength of 0.010-inch-thick René 41 sheet.<sup>(36)</sup> Several items in this table are of interest. First is the difference in strength levels, in tension, as a result of heat treatment. The low-temperature solution-treat-and-age sequence, A, results in significantly higher tensile properties than does the higher temperature cycle, C, when tested as heat treated. When these specimens were soaked for 10-20 hours at 1800 F prior to testing, this difference in strength was very much lessened. On the other hand, when they were soaked for 10-20 hours at 2000 F before testing, there was again a large difference in strength. Also of interest is the fact that the unaged specimens, B, were at least as strong as the aged specimens when tested after soaking for 20 hours at 2000 F.

Wlodek<sup>(26)</sup> found that L-605 was oxidized intergranularly when exposed at temperatures from 1600 to 2200 F. A more even distribution of sub-scale oxidation occurred when the specimen was in

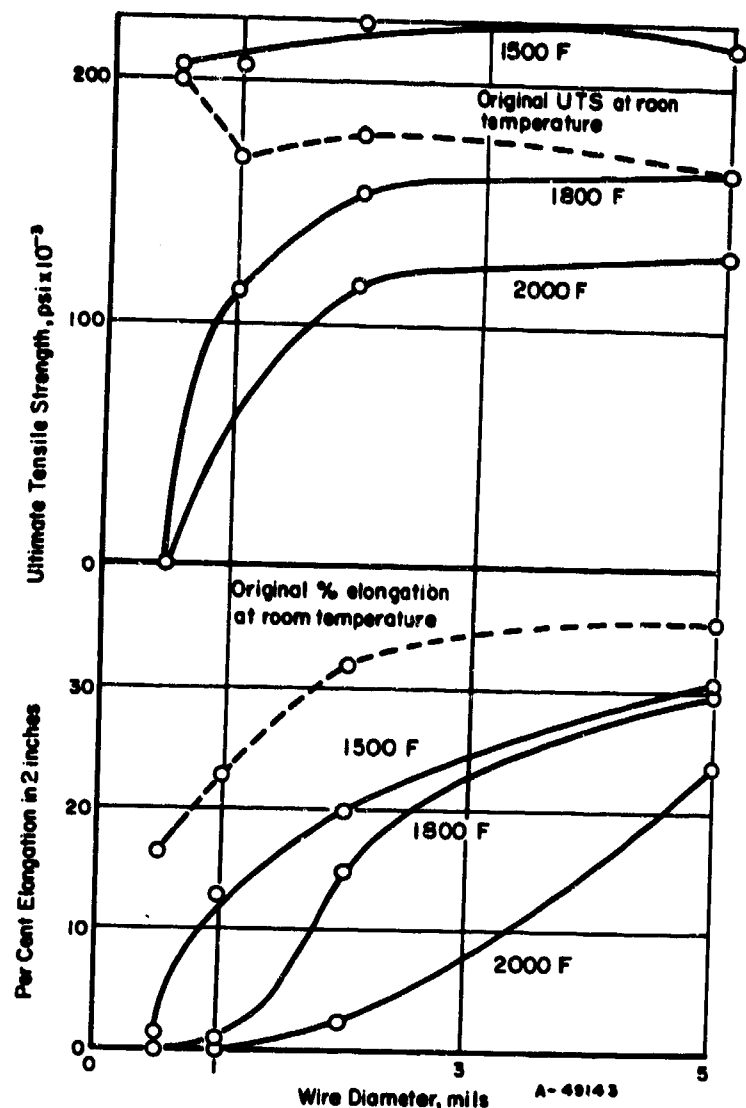


FIGURE 40. EFFECT OF RENÉ 41 WIRE DIAMETER ON LOSS IN STRENGTH AND DUCTILITY AFTER HEATING IN STATIC AIR FOR FIVE MINUTES<sup>(23)</sup>

TABLE 7. ROOM-TEMPERATURE MECHANICAL PROPERTIES OF RENÉ 41 AFTER SOAK AT ELEVATED TEMPERATURES<sup>(36)</sup>

Heat Treatment (a)	Test Condition	Ultimate Tensile Strength <sup>(b)</sup> , ksi	Yield Strength <sup>(b)</sup> , ksi	Elongation, %
A	No Soak	173	140	8
A	Soaked 1800 F, 10 hours	129	75	9
A	Soaked 2000 F, 10 hours	126	76	14
A	Soaked 1800 F, 20 hours	117	70	6
A	Soaked 2000 F, 20 hours	112	74	13
B	Soaked 2000 F, 20 hours	115	81	14
C	No Soak	131	112	4
C	Soaked 1800 F, 10 hours	110	77	9
C	Soaked 2000 F, 10 hours	76	59	5
C	Soaked 1800 F, 20 hours	106	72	8
C	Soaked 2000 F, 20 hours	64	54	5

(a) Heat-treatment code:

A - Solution treat 1950 F, age 1400 F

B - Solution treat 1950 F, no age

C - Solution treat 2150 F, age 1650 F.

(b) Calculated using material thickness before soak (original thickness 0.010 inch).

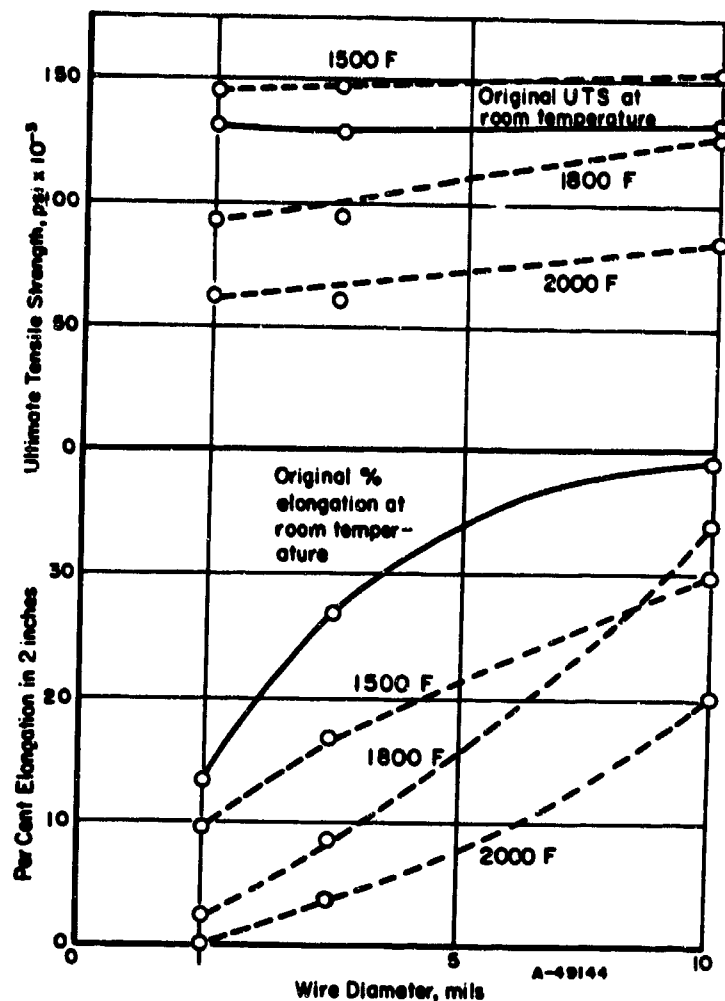


FIGURE 41. EFFECT OF INCONEL 702 WIRE DIAMETER ON LOSS IN STRENGTH AND DUCTILITY AFTER HEATING IN STATIC AIR FOR FIVE MINUTES<sup>(23)</sup>

the aged condition than when in the mill annealed condition. As-cast X-40 suffered internal oxidation mainly along the interdendritic areas. The average depths of internal oxidation in L-605 and X-40 observed in Wlodek's work and in other work (cited in Wlodek's report) are shown in Table 8.

TABLE 8. AVERAGE DEPTH OF INTERNAL OXIDATION IN L-605 AND X-40<sup>(26)</sup>

Alloy	Temp, F	Depth of Oxidation Per Side, mils		
		24 hr	100 hr	400 hr
L-605	1600	0.1	0.6	0.8
	1800	0.7	1.3	1.7
	2000	0.9	2.0	2.8
	2200	1.5	2.7	3.9
X-40	1600	0.2	0.5	1.0
	1800	0.8	1.5	2.2
	2000	1.6	3.1	3.9
	2200	1.3	2.2	3.7

### Alloy Depletion Effects

Intergranular oxidation is preceded by alloy depletion ahead of the advancing oxidation as seen in Figures 38 and 39. The compositional gradient that is produced can act as the driving force for continued metal-ion diffusion. The depleted zone also is weaker than the basic alloy, particularly in precipitation-hardenable nickel-base alloys where chromium, aluminum, and titanium are preferentially oxidized because of their relatively high affinity for oxygen. Loss of titanium and aluminum content is particularly detrimental to strength properties.<sup>(30, 32)</sup>

Malamand and Vidal made a study of alloy depletion by oxidation for various nickel-base alloys.<sup>(37)</sup> Their results for Nimonic 80 and Nimonic 95 are shown in Figures 42 through 45. Composition was determined spectrographically.

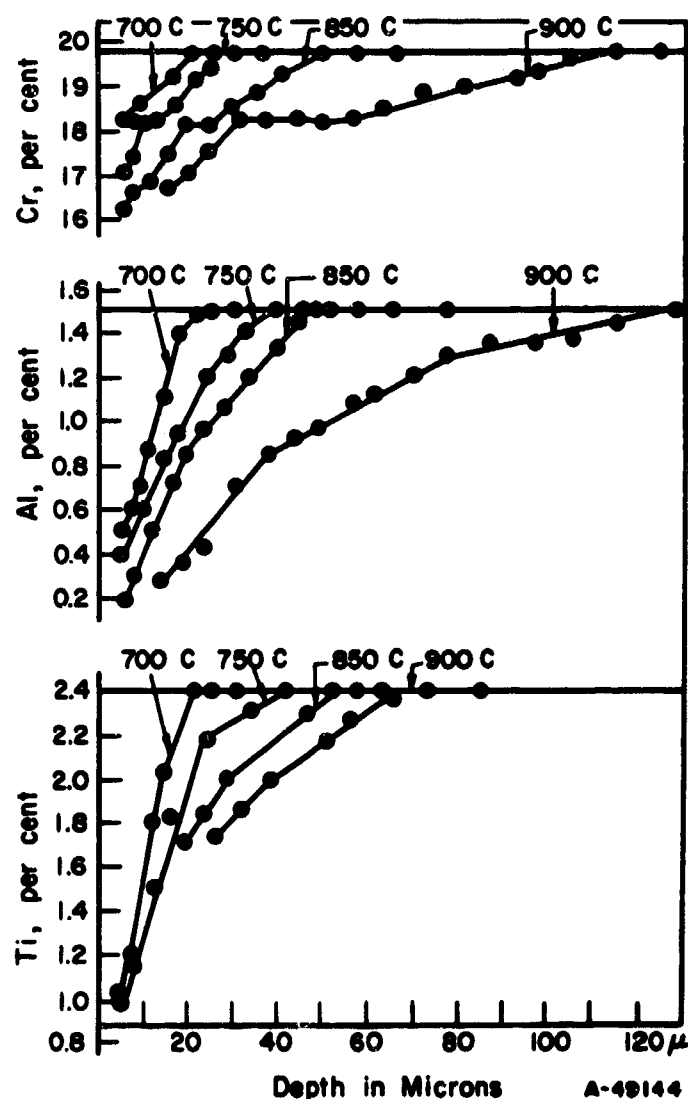


FIGURE 42. VARIATION OF CHROMIUM, ALUMINUM, AND TITANIUM CONTENTS IN NIMONIC 80 ALLOY OXIDIZED IN AIR AT TEMPERATURES BETWEEN 700 AND 900 C<sup>(37)</sup>

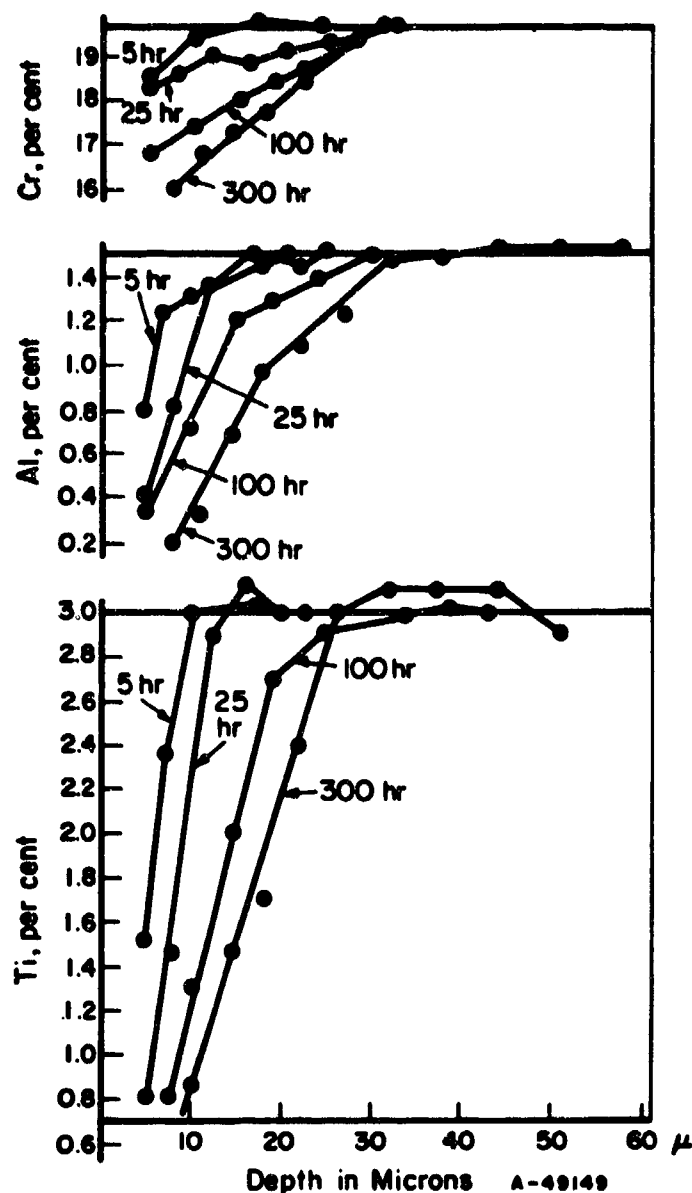


FIGURE 43. VARIATION OF CHROMIUM, ALUMINUM, AND TITANIUM CONTENTS WITH DEPTH BELOW THE SURFACE IN NIMONIC 95 ALLOY OXIDIZED IN AIR AT 800 C FOR 5, 25, 100, AND 300 HOURS<sup>(37)</sup>

Figure 42<sup>(37)</sup> shows the depletion of chromium, aluminum, and titanium in Nimonic 80 after 300 hours' exposure at various temperatures. Figure 43<sup>(37)</sup> shows the depletion of Nimonic 95 alloy as a function of time at 800 C (1475 F). The compositional gradients are quite steep even at short times. Figure 44<sup>(37)</sup> shows data on the depletion of various elements in Nimonic 95 after 300 hours at 800 C (1475 F), and the attendant decrease in hardness; note that cobalt is not depleted. Figure 45<sup>(37)</sup> is interesting because it represents a treatment often used on commercial hardware such as turbine blades. After machining, these parts are "skin annealed" in a salt bath to recrystallize the cold-worked areas.<sup>(37)</sup> A common practice is to heat the parts at 1080 C (1975 F)

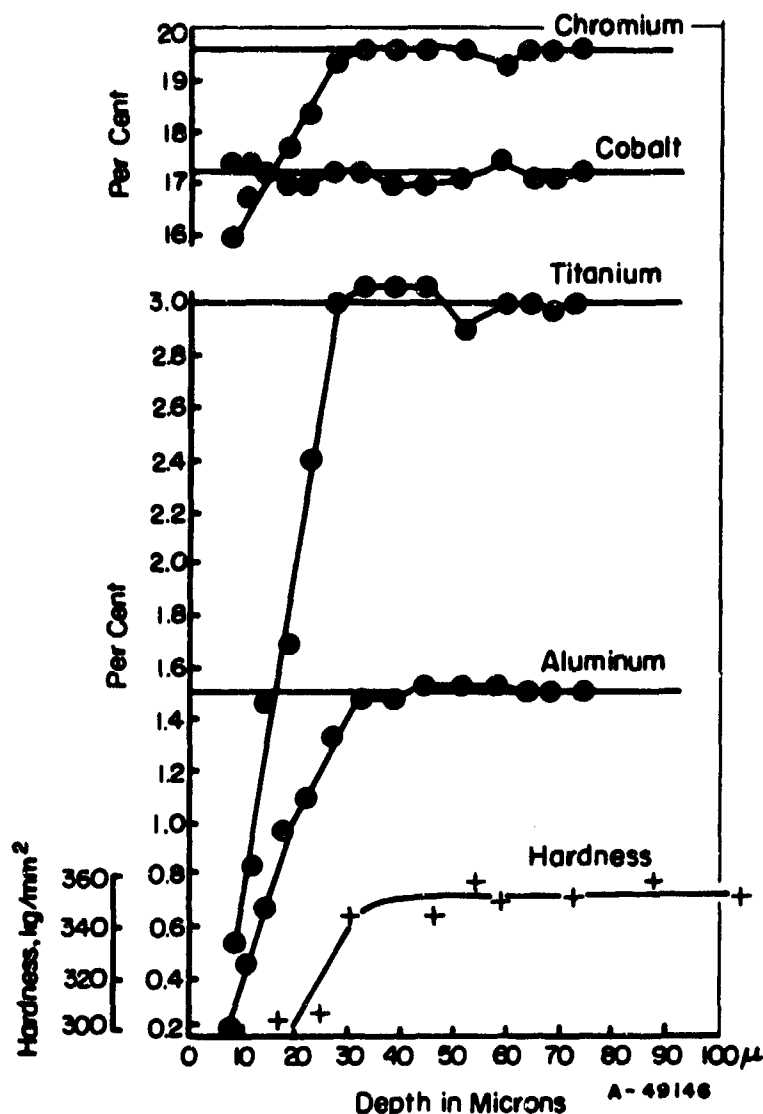


FIGURE 44. VARIATION OF CHROMIUM, COBALT, TITANIUM, AND ALUMINUM CONTENTS AND ACCOMPANYING HARDNESS OF NIMONIC 95 ALLOY OXIDIZED IN AIR AT 800 C FOR 300 HOURS<sup>(37)</sup>

for 10 minutes. Figure 45 shows that metal down to a depth of 100 microns (0.004 in.) is affected by depletion.

Wlodek's recent work<sup>(18, 16)</sup> on the oxidation of Hastelloy X, René 41, and Udimet 700 considers subscale reactions involving alloy depletion and internal oxidation. In René 41, Wlodek notes that the apparently intergranular attack (see Figure 33) below the scale does not follow prior grain boundaries, but penetrates along a network of newly formed subboundaries. He refers to this attack, which occurs with a different morphology in Hastelloy X and Udimet 700, as internal oxidation. Wlodek found that in René 41 and Udimet 700 the oxidation process occurs in three successive stages: formation of a thin film of  $\alpha\text{-Al}_2\text{O}_3$ , depletion of aluminum from the alloy adjacent to the oxide/metal interface, and oxidation of chromium

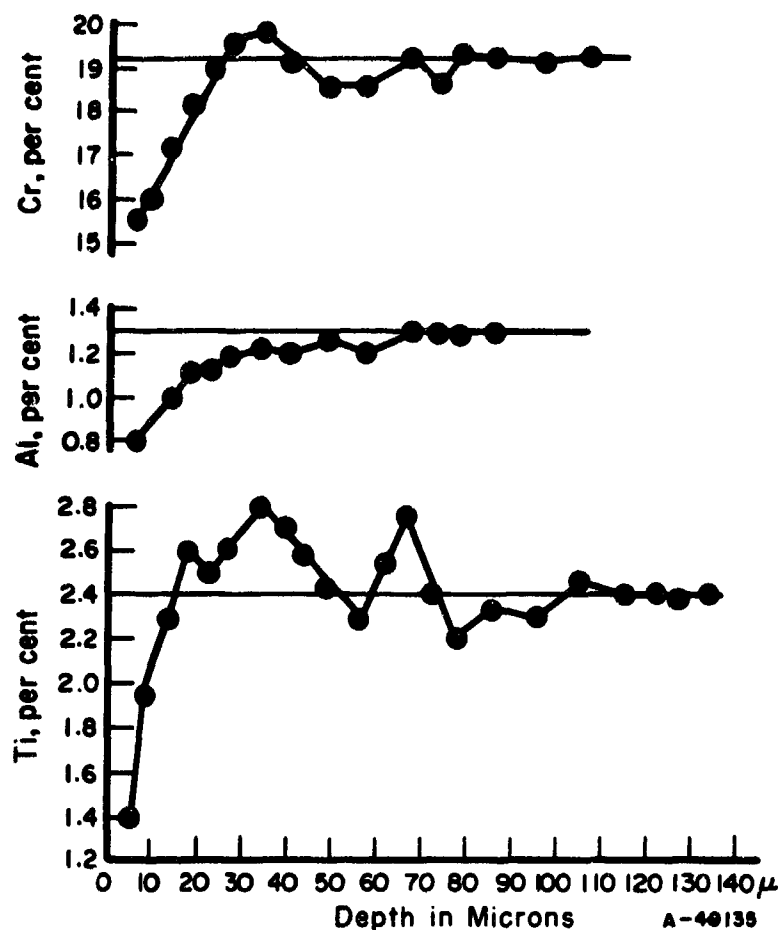


FIGURE 45. VARIATION IN CHROMIUM, ALUMINUM, AND TITANIUM CONTENTS IN NIMONIC 80 ALLOY AFTER "SKIN ANNEALING" FOR TEN MINUTES AT 1080 C (1975 F)<sup>(37)</sup>

by diffusion of  $\text{Cr}^{+3}$  along grain boundaries and through the nonthickening alumina layer. In Hastelloy X, a film of amorphous silica acts like the alumina film in the René 41, depleting silicon from the alloy, and requiring that further oxidation proceed by diffusion of  $\text{Cr}^{+3}$  and  $\text{Ni}^{+2}$ .

In X-40 and L-605, Wlodek<sup>(26)</sup> found that the alloy depletion effects were not pronounced enough to be observed reproducibly by etching. When observed, the depth of alloy depletion was roughly equivalent to the depth of internal oxidation.

#### OTHER SUBSURFACE OXIDATION

Some nickel-chromium-base alloys are subject to subsurface preferential oxidation, sometimes called green-rot. This has two distinguishing characteristics, namely, that a fractured surface has a definite green color, and that the metal area affected is magnetic because of the loss of chromium. Although this particular type of oxidation is not usually found in the superalloys, it is discussed here in order that it may be recognized if encountered.

This form of internal oxidation in nickel-base alloys is unpredictable, and no completely satisfactory model has been developed to explain its occurrence. Two general schools of thought exist. One ascribes the internal oxidation to the preferential oxidation of chromium rather than of nickel in atmospheres that are oxidizing to chromium and reducing to nickel.<sup>(38)</sup> Such atmospheres, of course, would exist only under special conditions, but this type of oxidation could also take place if the ambient atmosphere fluctuated between oxidizing and reducing.

Another school of thought holds that internal oxidation takes place most readily under a surface that had been previously carburized. It is considered that the chromium carbides formed as a result of the carburization are preferentially attacked. There have been many observations, made under industrial conditions, that tend to support this viewpoint.

It was concluded from a series of experiments by the International Nickel Company that the parameters for internal oxidation are not clearly defined.<sup>(39,40)</sup> It was found that internal oxidation took place more readily in areas that had been previously carburized, but that carburization was not a prerequisite. Areas not previously carburized also were attacked; however, ambient atmosphere was also found to be an important consideration, although its specific effect was not determined. Electron-probe microanalysis showed that the chromium content of the oxide and carbides of an oxidized specimen were indeed higher than the matrix (see Figure 46), thus supporting the concept of chromium depletion from the matrix.<sup>(40)</sup> However, these studies also showed that similar specimens could be made to oxidize internally, or not, by varying the temperature and composition of the ambient atmosphere. When carbon monoxide gas was used, no internal

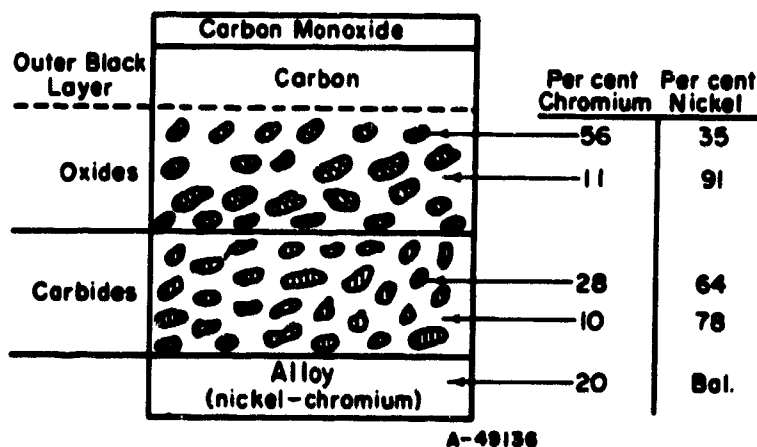


FIGURE 46. SCHEMATIC DIAGRAM OF ANALYSIS BY THE ELECTRON-PROBE MICROANALYZER<sup>(40)</sup>

oxidation occurred unless conditions permitted the dissociation of some CO to C and CO<sub>2</sub>. Under the conditions of the experiments, the optimum amount of carbon dioxide for producing internal oxidation was 3 to 13 per cent. Catalytic action accelerated the attack.

### EFFECT OF STRESS

Any discussion, however brief, on the problem of oxidation of superalloys should include some mention of the effect of stress on the oxidation behavior of the alloys. It is difficult, however, to present specific data because of the individual nature of the response of each alloy to the combined effects of oxygen, temperature, and stress. Data of this type are scarce, and data from different studies cannot be compared satisfactorily because of the wide variety of testing conditions. Data are sometimes generated ad hoc to satisfy a specific need, application, or design factor.

Some general ideas on the oxidation behavior of superalloys under stress were put forth in the work of Richmond and Thornton.<sup>(41)</sup> Table 9 and Figures 47 and 48 represent data extracted from their work. The depth of penetration was determined by observation of metallographic specimens. The most significant finding was that, at each temperature level, oxidation proceeded at a constant rate with increasing stress until a certain critical stress level was reached at which oxidation proceeded much more rapidly. Table 8 summarizes these data. Figures 47 and 48 show data plotted for Hastelloy Alloy R235. Similar curves can be drawn for the other alloys. In the examples shown, Hastelloy Alloy R235 begins to undergo accelerated oxidation at 1500 F when a stress level of about 23,000 psi is reached. At 1600, 1700, and 1800 F, the critical stress levels are about 15,000, 12,000, and 5,000 psi, respectively.

The increased oxidation rate can be explained in many ways, two of which are as follows: (1) increased diffusion rates occur within the stressed areas, thereby increasing the frequency with which metal and oxygen react and (2) at the

TABLE 9. STRESS AT WHICH DEPTH OF OXIDE PENETRATION BEGAN TO INCREASE RAPIDLY WITH STRESS IN SEVERAL NICKEL-BASE ALLOYS<sup>(41)</sup>

Alloy	Stress, psi, at Indicated Temperature, F							
	For Average Depth of External Oxide Penetration				For Maximum Depth of Oxide Penetration			
	1500	1600	1700	1800	1500	1600	1700	1800
Inconel 702	10,000	5,500	1,800	1350	10,000	5,500	2,000	1100
Hastelloy R235	23,000	15,000	12,000	5000	23,000	15,000	12,000	5000
Inconel X	20,000	17,500	15,000	7000	20,000	16,000	15,000	7000
Hastelloy W	15,000	8,500	2,000	700	15,000	8,500	2,000	700

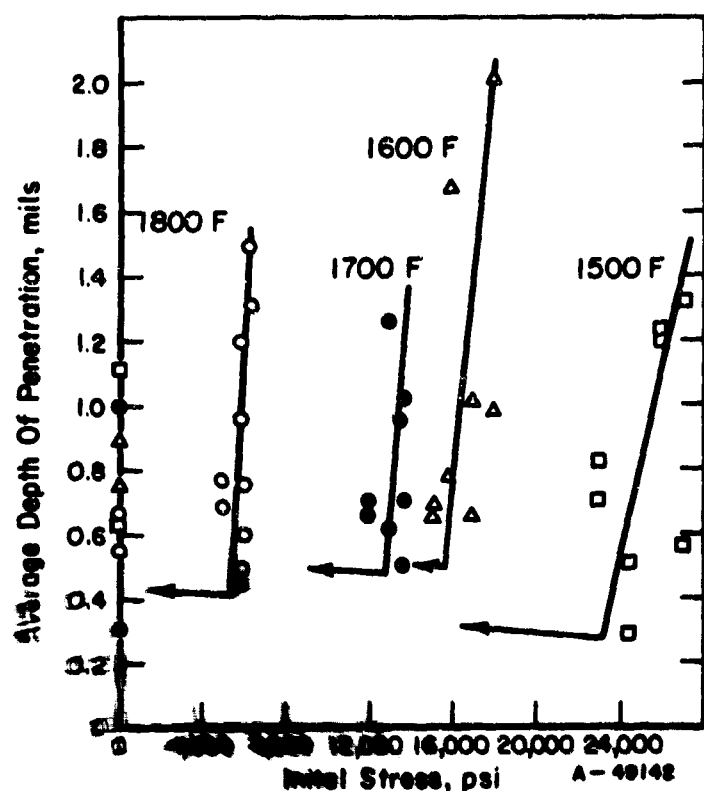


**FIGURE 47. PLOT OF AVERAGE DEPTH OF EXTERNAL OXIDATION OF HASTELLOY R235, AT FOUR TEMPERATURES AS A FUNCTION OF STRESS(41)**

Exposure time for all specimens was 100 hours.

critical applied stress the rate of metal deformation just exceeds the rate of growth of oxides. Protective oxides normally occupy a greater volume than the metal they displace, thus covering the metal with a self-healing layer that is in compression. If the metal underneath is being elongated at such a rate that the volume of oxide formed is not sufficient to keep up with the rate of expansion of the metal surface, the oxide will no longer be protective: fresh metal will be exposed as oxidation proceeds. In this regard an interesting observation was that the minimum stress to

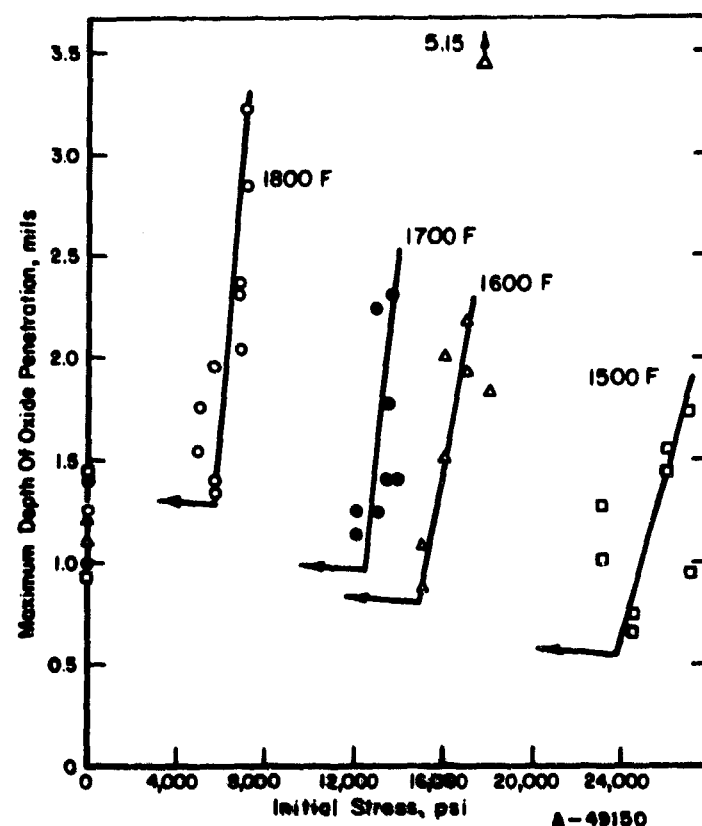


**FIGURE 48. PLOT OF MAXIMUM DEPTH OF OXIDE PENETRATION OF HASTELLOY R235 AT FOUR TEMPERATURES AS A FUNCTION OF STRESS(41)**

Exposure time for all specimens was 100 hours.

produce accelerated oxidation roughly corresponded to the stress necessary to produce 1 per cent extension in 100 hours.

Stress also is important from the standpoint of spalling. Although the surface oxides on most superalloys are tough tightly adherent layers that resist spalling, extensive deformation can produce sufficient shear at the metal-oxide interface to cause cracking and separation.<sup>(14)</sup> Under these conditions oxidation is rapid as fresh metal is continuously being exposed for further reaction.

## REFERENCES

- (1) Tumarev, A., and Panyushin, L., "Scale Resistance of Alloys of the Ternary System Nickel-Aluminum-Chromium", *Izvestiya Vysshikh Uchebnykh Zavedeniy-Chernaya Metallurgiya*, No. 9, pp 125-131 (1959).
- (2) Zima, G., "Some High Temperature Oxidation Characteristics of Nickel With Chromium Additions", *Transactions American Society for Metals*, 49, pp 924-947 (1957).
- (3) Phalnikar, C., Evans, E., and Baldwin, W., Jr., "High Temperature Scaling of Cobalt-Chromium Alloys", *Journal of Electrochemical Society*, 103 (8), 429-438 (1956).
- (4) Gulbransen, E. A., and McMillan, W. R., "Oxide Film on Nickel-Chromium Alloys", *Industrial and Engineering Chemistry*, 45, pp 1734-1744 (1953).
- (5) Ignatov, D., and Shamgunova, R., "Mechanism of Oxidation of Some Ni-Cr Base Alloys", *Izvestiya Akademii Nauk, SSSR, Otdel. Tekhn. Nauk, Metall. i Toplivo*, (3), pp 83-87 (1959).
- (6) Ignatov, D., and Shamgunova, R., "Structural-Kinetic Investigation into Oxidation Process of Nickel and Chromium and Alloys Based on Them", *Issledovaniya po Zharoprochnym Splavam*, 4, pp 346-351 (1959).
- (7) Kubaschewski, O. and Hopkins, B., *Oxidation of Metals and Alloys*, Academic Press, New York, New York, Second Edition (1962), 319 pp.
- (8) Hagel, W. C., "The Oxidation of Iron-, Nickel-, and Cobalt-Base Alloys Containing Aluminum", paper presented at the 2nd International Congress on Metallic Corrosion sponsored by the National Association of Corrosion Engineers, New York, New York, March 11-15, 1963.
- (9) "The Nimonic High Temperature Alloys", Engineering Data, Henry Wiggin and Company, Ltd, Holmer Road, Hereford, England (1960).
- (10) Betteridge, W., and Franklin, A., "Development of Ni-Cr-Base Alloys for High-Temperature Application", *Revue de Metallurgie, Memoires*, 53, pp 271-284 (1956).
- (11) Wood, D. R., "Investment-Cast Alloys for High-Temperature Service", *Foundry Trade Journal*, 106 (2275), 663-668 (June 4, 1959).
- (12) Preliminary Technical Data SM High Temperature Alloys, Sierra Metals Corporation (1962).
- (13) Eiselstein, H., and Skinner, E., "Effect of Composition on the Scaling of Iron-Chromium-Nickel Alloys Subjected to Cyclic Temperature Conditions", ASTM Special Technical Publication No. 165 (1954).
- (14) Kihlgren, T. E., "A Review of Nickel-Base Alloys for Aeronautical Applications", International Nickel Company.
- (15) Childers, M. G., and Simenz, R. F., "Clad Protection of Thin Sheet", Society of Automotive Engineers Paper 742E, September 23-27, 1963.
- (16) Wlodek, S. T., "The Oxidation of René 41 and Udimet 700", *Transactions of the Metallurgical Society of AIME*, 230, pp 1079-1090 (August 1964).
- (17) Rabensteine, A. S., "Oxidation Characteristics of Various Structural Materials for Ramjets and Heat Exchangers", Report PR 281-4Q-1, under Air Force Contract AF 33(657)-8706, The Marquardt Corporation, Van Nuys, California (June 15, 1963).
- (18) Wlodek, S. T., "The Oxidation of Hastelloy X", *Transactions of the Metallurgical Society of AIME*, 230, p 177 (February, 1964).
- (19) Manning, C. R., Jr., Royster, D. M., and Braski, D. N., "An Investigation of a New Nickel Alloy Strengthened by Dispersed Thorium", NASA Technical Note D-1944, Langley Research Center, Hampton, Virginia (July, 1963).
- (20) "TRW-1900 A High Strength Nickel-Base Superalloy for Use at High Temperatures", Preliminary Data Sheet of Thompson Ramo Wooldridge Inc., Cleveland, Ohio (March 25, 1963).
- (21) Austin, C. R., "High Temperature Properties of Ni-Co-Fe Base Age Hardening Alloys", *Transactions American Society of Metals*, 24, pp 481-512 (September, 1936).
- (22) Freche, J. C., and Waters, W. J., "Continued Investigation of an Advanced-Temperature, Tantalum-Modified, Nickel-Base Alloy", NASA Technical Note D-1531 (April, 1963).

- (23) Johnson, D., Newton, E., Benton, E., Ashman, L., and Knapton, D., "Metal Filaments for High Temperature Fabrics", ASD Technical Report No. 62-180, under Air Force Contract AF 33(616)-7294, Arthur D. Little, Inc., Cambridge, Massachusetts (February, 1962).
- (24) Ecker, L., and Huffman, J., "Final Report on Investigation of Sheet Alloys for Turbojet Engine Exhaust Systems", North American Report No. NA-48-400 (July 1, 1948).
- (25) Eberle, E., Hoke, J. H., Leyda, W. E., "Development of Cast Iron-Base Alloys of Austenitic Type for High Heat Resistance and Scale Resistance", WADC Technical Note 55-290, under Air Force Contract No. AF 33(616)-2413, The Babcock & Wilcox Company, Beaver Falls, Pennsylvania (January, 1957).
- (26) Wlodek, S. T., "The Oxidation of L-605 and X-40", Report R64FPD12, General Electric Company, Cincinnati, Ohio (January 24, 1964).
- (27) Dempsey, K. B., "Sheet Material for Service to 2700 F", Research Memorandum No. 8, Universal-Cyclops Steel Corporation, Bridgeville, Pennsylvania (January 13, 1956).
- (28) "SM302 High Temperature Cobalt-Base Superalloy", Sierra Metals Corporation, Wheeling, Illinois (1962).
- (29) MacFarlane, R., Pitler, R., and Reynolds, E., "Investigation of Forged Cobalt-Base Alloys for High Temperature Applications", WADC Technical Report No. 56-327, under Air Force Contract AF 33(616)-2882, Allegheny Ludlum Steel Corporation, Pittsburgh, Pennsylvania (October, 1956).
- (30) Lund, C., "Physical Metallurgy of Nickel-Base Superalloys", DMIC Report 153, Defense Metals Information Center, Battelle Memorial Institute, Columbus, Ohio (May 5, 1961).
- (31) Childers, M. G., and Koriagin, V. B., "Light Weight Structures for Space Vehicles", Society of Automotive Engineers Paper No. 420C, October 9-13, 1961.
- (32) Betteridge, W., "The Nimonic Alloys", Edward Arnold Ltd., London, 322 pp (1959).
- (33) Simenz, R., "This Test for Oxidation Resistance", Product Engineering, 30 (17), 48-50 (April 27, 1959).
- (34) Inco Current Data Report Number 5, International Nickel Company, New York, New York.
- (35) Dukes, W. H., Gosden, C., Kappelt, G., and Mirti, A. E., "Manufacturing Methods for Insulated and Cooled Double-Walled Structures", ASD TR-61-799, II, Section I, (1961).
- (36) "Strength Properties of René 41 After Short Time Exposure to High Temperature-Time Cycles", Report No. SRM 434, Preliminary Data, Lockheed Aircraft Corporation, Burbank, California (September 8, 1959).
- (37) Malamand, F., and Vidal, G., "Effects of High Temperature Oxidation on the Surface Composition of a Ni-Cr-Ti-Al Alloy", Comptes Rendus, 240, pp 186-188 (1955).
- (38) Spooner, N., Thomas, J., and Thomassen, L., "High Temperature Corrosion in Nickel-Chromium Alloys", Journal of Metals, 197, p 844 (June, 1953).
- (39) Copson, H., and Lang, F., "Some Experiments on Internal Oxidation of Nickel-Chromium Alloys", Corrosions, 15 (4), pp 194t-198t (April, 1959).
- (40) Hopkinson, B., and Copson, H., "Internal Carburization and Oxidation of Nickel-Chromium Alloys in Carbon Monoxide-Type Atmospheres, Corrosion, 16 (12), pp 608t-612t (1960).
- (41) Richmond, J., and Thornton, H., "Oxidation of Experimental Alloys", WADC Technical Report 58-164, Part I, under Air Force Contract AF 33(616)-56-19 National Bureau of Standards (June, 1958).



**APPENDIX**

**ALLOY INDEX AND COMPOSITIONS**

TABLE A-1. ALLOY INDEX AND COMPOSITIONS

Alloy	Composition, per cent															Other	Index Page No.
	Ni	Fe	Co	C	Mn	Si	Mo	W	Cb	Ta	B	Zr	Ti	Al	Cr		
80-20* (Nichrome V)	Bal.	0.28	--	0.06	--	1.12	--	--	--	--	--	--	--	--	19.8	6, 10, 11, 17	
80-20 + Mn*	Bal.	0.44	--	0.05	1.76	1.09	--	--	--	--	--	--	--	--	20.0	6	
Hastelloy Alloy R 235	Bal.	10.0	--	0.15	--	--	5.5	--	--	--	--	--	2.50	2.0	15.5	17, 18, 23, 24	
Hastelloy Alloy W	Bal.	--	--	0.1	--	--	25	--	--	--	--	--	--	--	5	0.6 V, max 23	
Hastelloy Alloy X	Bal.	20	1.5	0.10	--	--	9.0	0.6	--	--	--	--	--	--	22.0	8, 9, 17, 18, 22, 23	
IN-100	Bal.	--	15.0	0.18	--	--	3.0	--	--	0.015	0.05	5.0	5.5	10	1.0 V	5, 16	
Inconel(1)*	Bal.	7.91	--	0.04	0.25	0.37	--	--	--	--	--	--	--	--	16.4	7, 18	
Inconel (pre-1951)*	Bal.	6.67	--	0.06	0.23	0.32	--	--	--	--	--	--	--	--	14.1	6, 7	
Inconel W(6)	Bal.	6.5	--	0.04	--	--	--	--	--	--	--	2.4	0.6	15.0		7	
Inconel X(2)	Bal.	6.75	--	0.04	0.7	0.3	--	--	0.9	--	--	2.5	0.9	15.0		1, 7, 17, 18	
Inconel 702(3)	Bal.	0.35	--	0.04	0.05	0.20	--	--	--	--	--	0.70	3.40	15.6		7, 13, 17-20, 23	
K42B	Bal.	7.5	25	--	--	--	--	--	--	--	--	2.5	--	20		9-11	
Nicrotung	Bal.	--	10	--	--	--	--	8	--	--	0.05	0.05	4.0	4.0	12	11, 12	
Nimonic 75	Bal.	--	--	0.12	--	--	--	--	--	--	--	--	0.5	--	20	4, 6, 7	
Nimonic 80	Bal.	--	--	0.08	--	--	--	--	--	--	--	2.4	1.5	20		4, 21, 22	
Nimonic 80A	Bal.	--	--	0.08	--	--	--	--	--	--	--	2.4	1.5	20		4	
Nimonic 90	Bal.	--	17.5	0.10	--	--	--	--	--	--	--	2.4	1.6	20		4	
Nimonic 95	Bal.	--	17.5	0.12	--	--	--	--	--	--	--	3.0	2.0	20		4, 21, 22	
Nimonic 100	Bal.	--	20.0	0.20	--	--	5.0	--	--	--	--	1.3	5.0	11		4, 5	
Nimonic 105	Bal.	--	20.0	0.15	--	--	5.0	--	--	--	--	1.2	4.7	15		4, 5	
René 41	Bal.	--	11.0	0.09	--	--	10.0	--	--	--	0.005	--	3.1	1.5	19	1, 7-9, 11-13, 16-20, 22	
SM-200(7)	Bal.	0.25	10	0.15	--	--	--	12.5	1	--	0.15	0.05	2	5	9	5, 14, 16	
NASA Alloy TaZ8	Bal.	--	--	0.125	--	--	4	4	--	8	--	1	--	6	6	2.5 V 11, 12	
Thoriated Nickel	Bal.	--	--	--	--	--	--	--	--	--	--	--	--	--	--	2% ThO <sub>2</sub> by volume 9	
TRW-1930	Bal.	--	10	0.11	--	--	--	9	1.5	--	0.03	0.10	1	--	10.3	9	
Udimet 700	Bal.	--	18.5	0.10	--	--	5.2	--	--	--	0.008	--	3.5	4.3	15.0	7, 8, 22	
Cobalt-Base Alloys																	
AF-94	10	--	Bal.	0.12	--	--	5	10	1**	--	--	--	--	--	15	0.04 Be 14, 16	
Elgiloy	15	16	Bal.	0.15	2.0	--	7	--	--	--	--	--	--	--	20	13	
Haynes Stellite Alloy 21	2.5	--	Bal.	0.25	--	--	5.5	--	--	--	0.007, max	--	--	--	27	13, 14	
Haynes Stellite Alloy 31 (X-40)	10.5	--	Bal.	0.50	--	--	--	7.5	--	--	--	--	--	--	25.5	4, 13-16, 20, 22	
Haynes Alloy 25 (L-605)	10	--	Bal.	0.10	--	--	--	15	--	--	--	--	--	--	20	7, 13, 15-20, 22	
J-1570	28	--	Bal.	0.2	--	--	--	7	--	--	--	--	4	--	20	16	
S-816	20	3	Bal.	0.38	--	--	4	4	4**	--	--	--	--	--	20	13	
SM 302(8)	--	--	Bal.	0.85	--	--	--	10	--	9	0.005	0.20	--	--	22	14, 16	
WI 52	--	--	Bal.	0.45	--	--	--	11	2	--	--	--	--	--	21	14, 16	
X-40	See Haynes Stellite Alloy 31																
Iron-Base Alloys																	
AISI Type 304*	10.38	Bal.	--	0.06	1.58	0.48	--	--	--	--	--	--	--	--	17.37	7	
AISI Type 309*	13.18	Bal.	--	0.14	1.48	0.69	--	--	--	--	--	--	--	--	23.04	6, 7	
AISI Type 310*	25.70	Bal.	--	0.12	1.79	0.43	--	--	--	--	--	--	--	--	20.03	6, 7	
AISI Type 330*	35.0	Bal.	--	0.05	1.93	0.80	--	--	--	--	--	--	--	--	15.43	6, 7	
AISI Type 347*	10.70	Bal.	--	0.09	1.22	0.30	--	(0.9)***	--	--	--	--	--	--	17.82	7	
Incoloy*(4)	35.17	Bal.	--	0.04	0.85	0.52	--	--	--	--	--	--	--	--	20.20	6, 7	
Incoloy "T"*(5)	32.0	Bal.	--	0.04	0.75	0.35	--	--	--	--	--	--	1.0	--	20.50	7	
19-9 DL	10.0	Bal.	--	0.31	1.15	0.60	1.3	1.3	0.60**	--	--	--	0.25	--	19.0	0.5 Cu, max. 7	

- (1) New Designation by International Nickel Company: Inconel Alloy 600.  
 (2) New Designation by International Nickel Company: Inconel Alloy 601.  
 (3) New Designation by International Nickel Company: Inconel Alloy 602.  
 (4) New Designation by International Nickel Company: Inconel Alloy 603.  
 (5) New Designation by International Nickel Company: Inconel Alloy 604.  
 (6) New Designation by International Nickel Company: Inconel Alloy 722.

- (7) New Designation by Martin Metals MAR M 200.  
 (8) New Designation by Martin Metals MAR M 302.  
 \*Actual analysis from Reference 12.  
 \*\*Cb + Ti.  
 \*\*\*Was not given in analysis.

LIST OF DMIC TECHNICAL REPORTS ISSUED  
DEFENSE METALS INFORMATION CENTER  
 Battelle Memorial Institute  
 Columbus, Ohio 43201

Copies of the technical reports listed below may be obtained from DMIC at no cost by U. S. Government agencies, U. S. Government contractors, subcontractors, and/or their suppliers. Others may purchase copies of these reports from: Clearinghouse for Federal Scientific and Technical Information, U. S. Department of Commerce, Springfield, Virginia 22151. The CFSTI reference numbers (PB or AD prefix numbers) and prices are shown in parentheses. HC refers to Hard Copy price; Mf refers to Microfiche price. Orders to CFSTI should refer to the reference numbers and be prepaid.

Number	Title
*150	A Review of Bending Methods for Stainless Steel Tubing, March 2, 1961 (PB 151109, \$1.50)
151	Environmental and Metallurgical Factors of Stress-Corrosion Cracking in High-Strength Steels, April 14, 1961 (PB 151110, \$0.75)
152	Binary and Ternary Phase Diagrams of Columbium, Molybdenum, Tantalum, and Tungsten, April 28, 1961 (AD 257739, \$3.50)
*153	Physical Metallurgy of Nickel-Base Superalloys, May 5, 1961 (AD 258041, \$1.25)
154	Evolution of Ultrahigh-Strength, Hardenable Steels for Solid-Propellant Rocket-Motor Cases, May 25, 1961 (AD 257976, \$1.25)
155	Oxidation of Tungsten, July 17, 1961 (AD 263598, \$3.00)
156	Design Information on AM-350 Stainless Steel for Aircraft and Missiles, July 28, 1961 (AD 262407, \$1.50)
157	A Summary of the Theory of Fracture in Metals, August 7, 1961 (PB 181081, \$1.75)
*158	Stress-Corrosion Cracking of High-Strength Stainless Steels in Atmospheric Environments, September 15, 1961 (AD 266005, \$1.25)
159	Gas-Pressure Bonding, September 25, 1961 (AD 265133, \$1.25)
160	Introduction to Metals for Elevated-Temperature Use, October 27, 1961 (AD 268647, \$2.50)
161	Status Report No. 1 on Department of Defense Refractory Metals Sheet-Rolling Program, November 2, 1961 (AD 267077, \$1.00)
162	Coatings for the Protection of Refractory Metals from Oxidation, November 24, 1961 (AD 271384, \$3.50)
163	Control of Dimensions in High-Strength Heat-Treated Steel Parts, November 29, 1961 (AD 270045, \$1.00)
164	Semiaustenitic Precipitation-Hardenable Stainless Steels, December 6, 1961 (AD 274805, \$2.75)
165	Methods of Evaluating Welded Joints, December 28, 1961 (AD 272088, \$2.25)
166	The Effect of Nuclear Radiation on Structural Metals, September 15, 1961 (AD 265839, \$2.50)
*167	Summary of the Fifth Meeting of the Refractory Composites Working Group, March 12, 1962 (AD 274804, \$2.00)
168	Beryllium for Structural Applications, 1958-1960, May 18, 1962 (AD 278723, \$3.50)
169	The Effect of Molten Alkali Metals on Containment Metals and Alloys at High Temperatures, May 18, 1962 (AD 278654, \$1.50)
170	Chemical Vapor Deposition, June 4, 1962 (AD 281887, \$2.25)
171	The Physical Metallurgy of Cobalt-Base Superalloys, July 6, 1962 (AD 283356, \$2.25)
172	Background for the Development of Materials to be Used in High-Strength-Steel Structural Weldments, July 31, 1962 (AD 284265, \$3.00)
173	New Developments in Welded Fabrication of Large Solid-Fuel Rocket-Motor Cases, August 6, 1962 (AD 284829, \$1.00)
174	Electron-Beam Processes, September 15, 1962 (AD 287433, \$1.75)
175	Summary of the Sixth Meeting of the Refractory Composites Working Group, September 24, 1962 (AD 287029, \$1.75)
176	Status Report No. 2 on Department of Defense Refractory Metals Sheet-Rolling Program, October 15, 1962 (AD 288127, \$1.25)
177	Thermal Radiative Properties of Selected Materials, November 15, 1962, Volume I (AD 294345, \$3.00), Volume II (AD 294346, \$4.00)
178	Steels for Large Solid-Propellant Rocket-Motor Cases, November 20, 1962 (AD 292258, \$1.00)
179	A Guide to the Literature on High-Velocity Metalworking, December 3, 1962 (AD 403493, \$3.50)
180	Design Considerations in Selecting Materials for Large Solid-Propellant Rocket-Motor Cases, December 10, 1962 (AD 294695, \$2.00)
181	Joining of Nickel-Base Alloys, December 20, 1962 (AD 296174, \$2.00)
182	Structural Considerations in Developing Refractory Metal Alloys, January 31, 1963 (AD 419383, \$1.00)
183	Binary and Ternary Phase Diagrams of Columbium, Molybdenum, Tantalum, and Tungsten (Supplement to DMIC Report 152), February 7, 1963 (AD 407987, \$2.75)
184	Summary of the Seventh Meeting of the Refractory Composites Working Group, May 30, 1963 (AD 413567, \$1.75)
185	The Status and Properties of Titanium Alloys for Thick Plate, June 14, 1963 (AD 421029, \$1.50)
186	The Effect of Fabrication History and Microstructure on the Mechanical Properties of Refractory Metals and Alloys, July 10, 1963 (AD 423952, \$1.75)
187	The Application of Ultrasonic Energy in the Deformation of Metals, August 16, 1963 (AD 423562, \$2.25)
188	The Engineering Properties of Columbium and Columbium Alloys, September 6, 1963 (AD 426255, \$3.50)
189	The Engineering Properties of Tantalum and Tantalum Alloys, September 13, 1963 (AD 426344, \$2.50)
190	The Engineering Properties of Molybdenum and Molybdenum Alloys, September 20, 1963 (AD 426264, \$4.00)

\* DMIC supply exhausted; copies may be ordered from CFSTI.

<u>Number</u>	<u>Title</u>
191	The Engineering Properties of Tungsten and Tungsten Alloys, September 27, 1963 (AD 425547, \$2.75)
192	Hot-Cold Working of Steel to Improve Strength, October 11, 1963 (AD 425948, \$2.00)
193	Tungsten Research and Development Review, October 23, 1963 (AD 425474, \$1.50)
194	A Discussion of the Physical Metallurgy of the 18 Per Cent Nickel Maraging Steels, November 15, 1963 (AD 430082, \$0.75)
195	Properties of Coated Refractory Metals, January 10, 1964 (AD 433782, \$2.25)
196	Hydrogen-Induced, Delayed, Brittle Failures of High-Strength Steels, January 20, 1964 (AD 601116, \$3.00)
197	Cracking in High-Strength Steel Weldments - A Critical Review, February 7, 1964 (AD 438432, \$4.00)
198	The Mechanical Properties of the 18 Per Cent Nickel Maraging Steels, February 24, 1964 (AD 600427, \$2.75)
199	The Application of High Pressure in Metal-Deformation Processing - Report of an Informal Symposium of the Metalworking Process and Equipment Program, March 2, 1964 (AD 437328, \$2.00)
200	Vacuum Degassing in the Production of Premium-Quality Steels, March 11, 1964 (AD 601823, \$4.00)
201	U. S. Government Metalworking Processes and Equipment Program, March 18, 1964 (AD 600088, \$2.25)
202	The Effects of High-Pressure, High-Temperature Hydrogen on Steel, March 26, 1964 (AD 601389, \$2.00)
203	Explosive Forming of Metals, May 8, 1964
204	The Welding and Brazing of Alloy 718, June 1, 1964
205	The Effects of Heat-Treating and Testing Environments on the Properties of Refractory Metals, August 20, 1964
206	An Introduction to Magnesium Alloys, August 26, 1964
207	Current Methods of Fracture-Toughness Testing of High-Strength Alloys With Emphasis on Plane Strain, August 31, 1964
208	Metal Deformation Processing, Volume 1, A Survey Conducted as Part of the Metalworking Process and Equipment Program (MPEP), August 14, 1964
209	Second Status Report of the U. S. Government Metalworking Processes and Equipment Program, November 23, 1964
210	Problems in the Load-Carrying Application of High-Strength Steels, October 26-28, 1964
211	Premium-Quality Aluminum Castings, January 4, 1965
212	Department of Defense Refractory Metals Sheet Rolling Program, Status Report No. 3, January 26, 1965
213	Metal Removal by Electrochemical Methods and Its Effects on Mechanical Properties of Metals, January 7, 1965